



TECHNICAL UNIVERSITY OF LIBEREC  
Faculty of Textile Engineering ■

# STUDY ON USE OF ALIPHATIC POLYESTERS IN TISSUE ENGINEERING

## Diploma thesis

Study programme: N3106 – Textile Engineering  
Study branch: 3106T018 – Nonwoven and Nanomaterials  
Author: **Bc. Lucie Vejsadová**  
Supervisor: Ing. Petr Mikeš, Ph.D.



TECHNICKÁ UNIVERZITA V LIBERCI  
Fakulta textilní  
Akademický rok: 2013/2014

## ZADÁNÍ DIPLOMOVÉ PRÁCE

(PROJEKTU, UMĚLECKÉHO DÍLA, UMĚLECKÉHO VÝKONU)

Jméno a příjmení: **Lucie Vejsadová**  
Osobní číslo: **T12000503**  
Studijní program: **N3106 Textilní inženýrství**  
Studijní obor: **Netkané a nanovláknenné materiály**  
Název tématu: **Studium využití alifatických polyesterů v tkáňovém inženýrství**  
Zadávací katedra: **Katedra netkaných textilií a nanovláknenných materiálů**

### Z á s a d y p r o v y p r a c o v á n í :

- 1.) Vypracování rešerže na dané téma.
- 2.) Optimalizace a výroba PLCL vlákných vrstev na zařízení nanospider.
- 3.) Sledování degradačních produktů a vliv degradace na změnu molekulové hmotnosti měřené pomocí gelové chromatografie.
- 4.) Diskuze výsledků, vyhodnocení dosažených výsledků.

Rozsah grafických prací:

Rozsah pracovní zprávy:

Forma zpracování diplomové práce: **tištěná/elektronická**

Seznam odborné literatury:

- 1) Fernández, J., et al., 2012. Synthesis, structure and properties of poly(L-lactide-co-e-caprolactone) statistical copolymers. *Journal of the Mechanical Behavior of Biomedical Materials*, September, pp. 100-112.
- 2) Albertsson, A. C., et al., 2002. *Degradable Aliphatic Polyesters*. Germany: Springer.
- 3) Ebnesajjad, S., 2013. *Handbook of Biopolymers and Biodegradable Plastics: Properties, Processing, and Applications*. United States: Elsevier.
- 4) Schnabel, W., *Polymer Degradation Principles and Practical Applications*, ISBN: 3-446-13264-3, 1981, 227 s.

Vedoucí diplomové práce:

**Ing. Petr Mikeš, Ph.D.**

Katedra netkaných textilií a nanovláknenných materiálů

Datum zadání diplomové práce: **17. června 2014**

Termín odevzdání diplomové práce: **14. května 2015**



Ing. Jana Drašarová, Ph.D.  
děkanka



prof. RNDr. David Lukáš, CSc.  
vedoucí katedry

V Liberci dne 17. června 2014

## **Declaration**

I hereby certify that I have been informed the Act 121/2000, the Copyright Act of the Czech Republic, namely § 60 - Schoolwork, applies to my master thesis in full scope.

I acknowledge that the Technical University of Liberec (TUL) does not infringe my copyrights by using my master thesis for TUL's internal purposes.

I am aware of my obligation to inform TUL on having used or licensed to use my master thesis; in such a case TUL may require compensation of costs spent on creating the work at up to their actual amount.

I have written my master thesis myself using literature listed therein and consulting it with my thesis supervisor and my tutor.

Concurrently I confirm that the printed version of my master thesis is coincident with an electronic version, inserted into the IS STAG.

Date:

Signature:

## **Acknowledgment**

I wish to express my thanks to my supervisor Ing. Petr Mikeš, Ph.D. for providing valuable advice and substantive comments during the preparation of this thesis. I am also grateful to the department faculty members for their help and support, especially to Ing. Aleš Šaman for his professional advice, and to Ing. Věra Jenčová, Ph.D. for helpful assistance in laboratories and for the development of the experimental part of this work.

I would like to express my special appreciation and many thanks to my external advisor Dr Paul D. Topham for allowing me to grow in research. He has been a tremendous mentor for me. I would also like to thank Dr Gwen F. Chimonides and Robyn E. Powell for encouraging me on this journey. Your advices on the research as well as on my career have been priceless.

A special thanks go to my family and my friends who supported me in writing. I am also grateful to Kamila Boudová for English correction and for great motivation towards my goal.

## **Abstract**

This thesis studies the copolymer of aliphatic polyester, which could be a suitable material for applications in tissue engineering. Successful imitation of natural tissues is a decisive parameter for efficient tissue regeneration. Copolymer poly(lactide-co-caprolactone), could be a suitable material for solving this problem. In this work nanofibre layers were produced by electrospinning. These layers were subsequently subjected to degradation assay with applications of the enzyme proteinase K. The result was the detection of mass loss, change in the molar mass and the morphological changes of the fibres.

### **Keywords**

Aliphatic polyesters, degradation, electrospinning, poly(lactide-co-caprolactone), nanofibres

## **Abstrakt**

Tato diplomová práce se zabývá studiem alifatických polyesterů a možností jejich využití v tkáňovém inženýrství. Úspěšnost napodobování přirozených tkání je rozhodující parametr pro účinnou regeneraci. Slibným kandidátem pro tyto aplikace se jeví kopolymer poly(laktid-co-kaprolakton), který byl použit pro experimenty této práce. Z něj byly připraveny nanovláknenné vrstvy metodou elektrostatického zvláknování. Zkoumala se především otázka biodegradace tohoto kopolymeru. Za tímto účelem byly provedeny enzym-degradační testy katalyzované pomocí proteinázy K. Výsledkem byly hmotnostní úbytky materiálu a s tím související změny molekulových hmotností. Degradace kopolymeru byla potvrzena i morfologickými změnami vláken.

### **Klíčová slova**

Alifatické polyestery, degradace, elektrostatické zvláknování, poly(laktid-co-kaprolakton), nanovláknena

# Contents

List of Figures .....	9
List of Tables .....	10
Abbreviations.....	11
Introduction.....	12
1 Tissue Engineering .....	13
1.1 Biomaterials for Tissue Engineering.....	14
2 Biodegradable Polymers.....	16
2.1 Naturally Occurring Polymer Biomaterials .....	16
2.2 Synthetic Polymers.....	17
2.2.1 Aliphatic Polyesters .....	18
2.3 Production of Polylactide, Polycaprolactone and Their Copolymers .....	22
2.3.1 Polycondensation .....	22
2.3.2 Ring-Opening Polymerization .....	23
2.3.3 Copolymerization.....	24
2.4 Biodegradation .....	25
2.4.1 Factors Affecting Degradation.....	26
2.4.2 Degradation of aliphatic polyesters .....	27
3 Characterization of Polymers .....	30
3.1 Determination of Molar Mass Distributions .....	30
3.1.1 Gel Permeation Chromatography .....	31
3.2 Nuclear Magnetic Resonance Spectroscopy .....	33
4 Electrospinning.....	36
4.1 Electrospinning Process Parameters .....	36
4.1.1 Polymer Solution Parameters.....	37
4.1.2 Processing Parameters .....	38
4.1.3 Environmental Parameters .....	38

5	Experimental Part .....	39
5.1	Characteristics of Polyester Copolymers .....	39
5.1.1	Detection of Molar mass by GPC .....	39
5.1.2	<sup>1</sup> H NMR Characterization.....	42
5.1.3	Electrospinning Process Optimization.....	45
5.1.4	Surface Morphology Observed by SEM.....	46
5.2	Proteinase K-catalyzed Enzymatic Degradation .....	48
5.2.1	Materials and Methods.....	48
5.2.2	Amount Optimization of Enzyme.....	49
5.2.3	Degradation Study with 5 U/ml of Proteinase K .....	53
	Discussion.....	58
	Conclusion .....	59



## List of Figures

<b>Figure 1</b> <i>The principle of tissue engineering</i> .....	14
<b>Figure 2</b> <i>Chemical structure of PGA (Dimitrios, 2013)</i> .....	19
<b>Figure 3</b> <i>Chemical structure of PLA (Dimitrios, 2013)</i> .....	19
<b>Figure 4</b> <i>Chemical structure of PCL (Dimitrios, 2013)</i> .....	20
<b>Figure 5</b> <i>Chemical structure of PLCL (Dimitrios, 2013)</i> .....	21
<b>Figure 6</b> <i>Schematic representation of the ROP of a cyclic ester</i> .....	24
<b>Figure 7</b> <i>Illustration of alternating, block, random and graft copolymers</i> .....	25
<b>Figure 8</b> <i>Gel permeation chromatography analysis system</i> .....	31
<b>Figure 9</b> <i>The size separation mechanism of GPC</i> .....	32
<b>Figure 10</b> <i>Scheme of GPC device</i> .....	33
<b>Figure 11</b> <i>NMR Spectroscopy Analyser (Azom, 2011)</i> .....	34
<b>Figure 12</b> <i>Molar mass distribution of PLCL copolymers</i> .....	41
<b>Figure 13</b> <i><sup>1</sup>H NMR spectrum of PLCL_th_1</i> .....	43
<b>Figure 14</b> <i>SEM images of fibres structure of a) PLCL_p, b) PLCL_th_1, magnification 1000x, scale 50 μm</i> .....	47
<b>Figure 15</b> <i>Histogram of PLCL_p</i> .....	47
<b>Figure 16</b> <i>Histogram of PLCL_th_1</i> .....	48
<b>Figure 17</b> <i>Mass loss of PLCL with 10 U/ml and 20 U/ml of enzyme</i> .....	49
<b>Figure 18</b> <i>Molar mass loss with 10 U/ml and 20 U/ml of enzyme</i> .....	51
<b>Figure 19</b> <i>SEM images of PLCL_p with 10 U/ml (a, b) and 20 U/ml (c, d) of enzyme after 1 day and 2 day of degradation, magnification 1000x, scale 50 μm</i> .....	52
<b>Figure 20</b> <i>SEM images of PLCL_th_1 with 10 U/ml (a, b, c) and 20 U/ml (d, e, f) of enzyme after 1, 2 and 3 day of degradation, magnification 3000x, scale 20 μm</i> .....	53
<b>Figure 21</b> <i>Mass loss of PLCL with 5 U/ml of enzyme</i> .....	54
<b>Figure 22</b> <i>Molar mass loss with 5 U/ml of enzyme</i> .....	55
<b>Figure 23</b> <i>SEM images of PLCL_p with 5 U/ml of enzyme after 1 day (a), 2 day (b), 3 day (c) and 4 day (d), magnification 3000x, scale 20 μm</i> .....	56
<b>Figure 24</b> <i>SEM images of PLCL_th_1 with 5 U/ml of enzyme after 1 day (a), 2 day (b), 3 day (c) and 4 day (e), magnification 3000x, scale 20 μm</i> .....	57

## List of Tables

<b>Table 1</b> <i>Comparison between synthetic and natural polymers</i> .....	16
<b>Table 2</b> <i>Electrospinning process parameters (Mitpuppatham, et al., 2004)</i> .....	37
<b>Table 3</b> <i>Molar masss of copolymer granules</i> .....	40
<b>Table 4</b> <i>Molar ratio of LA:LC detected by <sup>1</sup>H NMR</i> .....	44
<b>Table 5</b> <i>Chain microstructure - monomer alternation</i> .....	44
<b>Table 6</b> <i>Nanospider TM process conditions</i> .....	46
<b>Table 7</b> <i>Molar mass loss with 10 U/ml and 20 U/ml of enzyme</i> .....	50
<b>Table 8</b> <i>Molar mass loss with 5 U/ml of enzyme</i> .....	55

## Abbreviations

$^1\text{H}$ NMR	Proton hydrogen nuclear magnetic resonance
ADSCs	Adipose-derived stem cells
CDCL <sub>3</sub>	Deuterated chloroform
ECM	Extracellular matrix
GPC	Gel permeation chromatography
LA	Lactide
LC	Lactone
Mn	Number average molar mass
Mw	Weight average molar mass
PBS	Phosphate buffered saline
PCL	Poly( $\epsilon$ -caprolactone)
PDI	Polydispersity index
PGA	Poly(glycolic acid)
PHB	Poly(hydroxybutyrate)
PHV	Poly(hydroxyvalerate)
PLA	Poly(lactide acid)
PLCL	Poly(lactide-co-caprolactone)
PTFE	Polytetrafluorethylene
RI	Refractive index
ROP	Ring-opening polymerisation
rpm	Revolutions per minute
SD	Standard deviation
TE	Tissue engineering
TERM	Tissue engineering and regenerative medicine
Tg	Glass transition temperature
Tm	Melting temperature
TMS	Tetramethylsilane
UV	Ultraviolet
v/v	Volume/volume
w/w	Weight/weight
$\delta$	Chemical shift

## Introduction

Polymers are a normal part of everyday life. They are used for production of a wide variety of objects and find application in many industry sectors. One of the key industries where the polymeric materials recently have recorded the most outstanding application is the field of medicine. The advantage of polymers compared to such as metal, glass or ceramics, which is the traditional materials in medicine, is particularly good compatibility with living tissue, ease of treatment and often lower cost. Classical polymer materials are being constantly improved by polymer chemistry and physics and at the same time brand new materials are being developed. Beside of traditional materials polymers include active materials which are able to mimic to a certain extent the behaviour of biological tissues or whole organisms. It turns out that the synthetic polymers can carry information and perform specific functions in the same way that the natural macromolecules do.

The aim of this theses was to produce a fibre layers from poly(lactide-co-caprolactone) copolymers by electrospinning. These layers went through the enzymatic-catalysed degradation tests. Subsequently, their degradation products were investigated in three ways, namely mass loss, changing of the molar mass and ultimately imaging morphological changes using scanning electron microscopy.

The first part of the paper describes the process of tissue engineering, the attributes and behaviour of synthetic polymers, their degradation characteristics and the test methods that were used in the evaluation of the experiments. The experimental part contains the exact procedure of manufacturing fibre layers and the way the degradation experiments were carried out, including all the obtained knowledge and evaluation.

# 1 Tissue Engineering

Tissue engineering (TE) also referred to as tissue engineering and regenerative medicine (TERM) can be applied to biological, chemical, medical and engineering principles leading to the recovery, restoration or regeneration of tissues, which has led to a new term regenerative medicine. One of the major goals of tissue engineering is the design of biomaterial scaffolds that allows regeneration of functional tissue in the host as an alternative to conventional organ transplantation and tissue reconstruction methods (Brown, 2013).

Nanotechnology and nanomaterials can also contribute to reproduction or reparation of damaged tissue. These functions are highly sought after since some traditional implants can be rejected by the body and transplantation methods have large limitations in general. The major problem is accessing enough tissue and organs for all of the patients who need them. It is within this context that the field of tissue engineering has emerged. In essence, tissue engineering develops a functional foundation called scaffolds on which the cells are grown in optimal case (Brown, 2013). With suitable modifications applied on traditional materials their physic-chemical characteristics are optimized in order to facilitate the interaction between the cell and the material. This leads to greater adhesion, growth, differentiation, and viability of totipotent cells. There are so many potential applications to tissue engineering that the overall scale is enormous (e.g. blood vessels, skin, bone, cartilage, muscle or nerve tissue) (Lanza, et al., 2014).

Scaffolds are able to establish three-dimensional environments for dissemination cells and can mimic native extracellular matrix (ECM). In general, the scaffolds can be divided into two strategies, (1) seeding of scaffold with living host cells before implantation (*cellular strategy*) and (2) unseeded scaffold (*acellular strategy*). Regarding the cellular strategy, the basic principle of TE is shown below in Figure 1. The process begins by taking a sample of autologous cells. The cultivation of these cells is carried out in laboratory conditions in vitro where proliferation is supported. During this process, a scaffold is created with required properties. Once the cells get to the desired quantity, they are applied to the scaffold, whereby they proliferate. After a while the seeded scaffold is implanted into the patient's body at the site

of the affected area. The cells contained in the scaffold will unite with the tissue at the implantation site which promotes infiltration and growth of new tissue, while the material of scaffold gradually degrades in vivo (Lanza, et al., 2014).

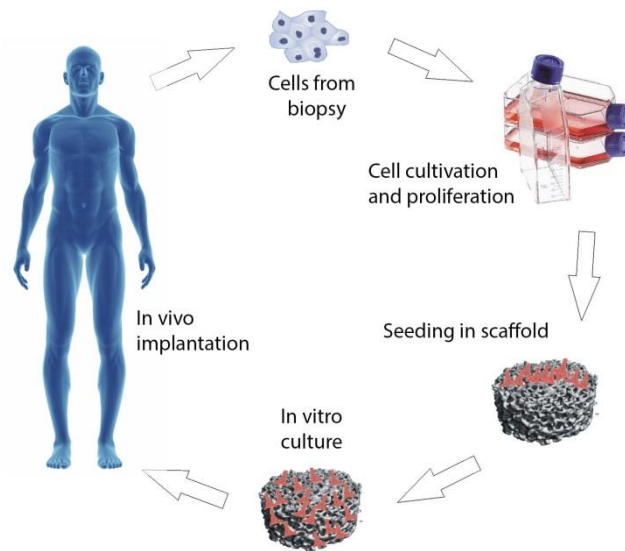


**Figure 1** The principle of tissue engineering

The second option is implanting an unseeded scaffold (*acellular strategy*). Acellular tissue matrices are usually prepared by removing cellular components from tissues. They retain the three-dimensional structure of authentic ECM which improves cell migration. Recently, Lanza and et al. (2014) has begun to test unseeded biomimetic scaffolds (Lanza et al., 2014; Chen, et al., 2013).

## 1.1 Biomaterials for Tissue Engineering

The types of biomaterials used in medical applications and devices include metals, ceramic and glasses, a wide range of natural and synthetic polymers or composites (Donglu, 2006). One of the main benefits of polymers compared with metals or ceramics are their desirable physical-mechanical properties, achievement of desired shape, adequate price, ability to support the growth of cells and in case of certain polymers, the biodegradability (Donglu, 2006; Lukáš, et al., 2008).

Biodegradable materials must comply with stringent requirements in comparison to nondegradable materials. Key issues include the biocompatibility, the possibility

of the toxic contaminants as a result of secretion of residual monomers among other and metabolic residues (Rui & Román, 2005). Biomedical polymers must be patterned with respect to physiological functions and conditions to which they will be exposed to in the organism. Because immediately after the surgical placement in vivo the polymer is likely to change its physical properties, such as mechanical strength or porosity (Lanza, et al., 2014).

## 2 Biodegradable Polymers

Polymer materials have been utilised in applications in every specialty area and played major role health care (He, et al., 2008). Polymers can be divided in several different groups according to their sources (natural and synthetic), chain structures, physical properties or their technological use. The advantages and disadvantages for synthetic and natural (naturally occurring) polymers are summarized in Table 1 (Bhat, 2005).

**Table 1** Comparison between synthetic and natural polymers (Bhat, 2005)

<b>Polymer</b>	<b>Advantages</b>	<b>Disadvantages</b>
<b>Synthetic</b>	Easily synthesized with controlled molar mass and other physical properties – for example mechanical properties	Lack of intrinsic biological activity
<b>Natural</b>	Possess intrinsic biological activity, Enzymatically degradable	Source-related variability and contamination, Limited control over parameters such as molar mass. Potential for adverse immunological responses. Variation in degradation rates due to difference in host enzyme levels. Inferior mechanical properties.

The division between polymers created by living organisms and man-made materials are not always clear cut. For example, poly (glycolic acid) is naturally produced by many organisms but can also be created synthetically from petroleum. The result is the same final product (Lanza, et al., 2014).

### 2.1 Naturally Occurring Polymer Biomaterials

Naturally occurring polymers are used for their structures similar to human tissue and plentiful resources, can degrade by naturally occurring enzymes and during degradation do not produce toxins. They are produced by biological processes within plants (e.g. Cellulose, Starch) and animals (e.g. Chitin, Keratin, and Elastin) (Bhat, 2005).



The biologically derived polymers can be additionally classified into: a) peptides and proteins, b) polysaccharides (Lanza, et al. 2014; Donglu, 2006).

Peptides and proteins are polymers consisted of amino acids connected via stable amide bonds. Therefore, these materials are usually degraded by enzymatic mechanism. The main shortcoming of these materials is their lack of process ability and their inherent immunogenicity as biomaterial. For example, in the past the safety of using bovine collagen has been discussed, as it causes an immune response and predisposes the patient to autoimmune diseases. Despite a number of disadvantages it may help to design a polymer with desirable characteristics for tissue engineering (Lanza, et al., 2014).

Polysaccharides are polymers made of various monosaccharide units; the most common are glucose and fructose (Lanza, et al., 2014). Most of the natural polysaccharides are not biodegradable in mammalian species for its lack of digestive enzymes. Therefore without additional chemical modification, most polysaccharides are not evident materials for biomedical applications (Bhat, 2005).

## **2.2 Synthetic Polymers**

Synthetic polymers are large molecular compounds made up by the repetition of small units termed monomers. In contrast to some of naturally derived polymers, synthetic polymers can be fabricated and their characteristics controlled for different applications. Due to this fact, synthetic materials have gradually replaced natural materials for wound closure purpose (Bhat, 2005).

Synthetic polymers can be divided into two large groups: a) non-biodegradable polymers, b) biodegradable polymers. In healthcare, non-biodegradable materials are mainly developed for non-biomedical use. They are often applied in hard connective tissue, such as artificial bones and joints, where the biodegradability is not a positive property. Non-biodegradable polymers used in biomedical applications include e.g. poly(propylene), poly(tetrafluoroethylene), poly(methylmethacrylate), poly(ethylene), etc. (Donglu, 2006; Bhat, 2005).

## 2.2.1 Aliphatic Polyesters

Polyester is a polymer category made of two main “groups” - aliphatic (linear) polyesters and aromatic (aromatic rings) polyesters (Nampoothiri, et al., 2010). Aliphatic polyesters, such as poly(hydroxybutyrate) (PHB), poly(hydroxyvalerate) (PHV), poly(glycolic acid) (PGA), poly(lactic acid) (PLA), poly( $\epsilon$ -caprolactone) (PCL), etc. have been utilized in clinical use since 1969 (Dimitrios, 2013). Because the work focuses on polyesters employed in tissue engineering, only characteristics and parameters of polymers PGA, PLA, PCL and their copolymers are described in this work.

These biodegradable polymers have hydrolysable ester bonds -CO(O)- in main chain. These are cleaved by hydrolysis and decrease molar mass of the implant. An initial degradation reduces the molar mass of oligomer over 5,000 Da (Dalton, atomic mass unit), where the oligomer becomes water soluble. Final degradation may cause an appearance of inflammatory cells at the site of application. The lifetime of polyester polymers is determined by the initial molar mass, surface area, crystallinity and in the case of copolymers by ratio of the monomers and by their structural chain (Donglu, 2006; Lanza, et al., 2014).

### **Poly(glycolic) acid**

Poly(glycolic) (PGA) (Figure 2) acid is the simplest linear aliphatic polyester. PGA is highly crystalline (45 % - 50 %), it has a glass transition temperature ( $T_g$ ) of 35 °C – 40 °C and a high melting point ( $T_m$ ) 220 °C – 225 °C. It is not soluble in most organic solvents. PGA has been used for absorbable suture. Due to its hydrophilic characteristic and quick water absorption, surgical suture lose 50% of its mechanical strength after two weeks and 100 % after four weeks, and finally it is completely absorbed in four to six months from implantation (Donglu, 2006; Lanza, et al., 2014).

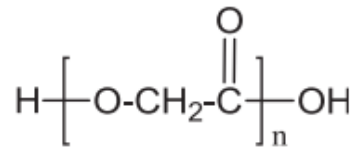


**Figure 2** Chemical structure of PGA (Dimitrios, 2013)

### **Poly(lactic) acid**

Poly(lactic) acid (PLA) or polylactide (Figure 3) exists in three forms: poly(D-lactide) (PDLA), poly(L-lactide) (PLLA) and poly(DL-lactide) (PDLLA). PDLA and PLLA are crystalline polymers, a glass transition temperature ( $T_g$ ) is approximately 60 °C, a peak melting temperature ( $T_m$ ) is around 180 °C. PDLLA is amorphous (Lanza, et al., 2014). As one of the few polymers, PLA can be modified simply by mixing L and D isomers. The polymer can therefore achieve higher molar mass and changes its crystallinity, which leads to a substantial impact of the degradation process (Ebnesajjad, 2013).

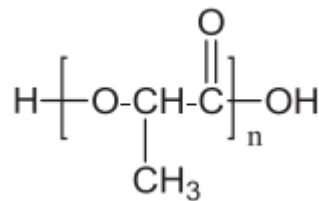


**Figure 3** Chemical structure of PLA (Dimitrios, 2013)

PLLA and PDLA are used for their high tensile strength and Young's modulus in orthopaedic fixation and sutures. It needs modification for most applications because of its brittleness. This poorness may be improved by blending or copolymerization with lower glass transition temperature polymers, e.g. poly( $\epsilon$ -caprolactone) (PCL) (Yu, et al., 2010). The adhesion forces of PLA-PCL blends are too weak to improve the desired stress transmission but their copolymers can accelerate the degradation rate of PCL and reduce the acidity of PLA (Fernández, et al., 2012a). These polymers degrade by hydrolysis and form lactic acid, which is normally presented in human body (PDLA has a much higher degradation rate than PLLA). The final product of the degradation is carbon dioxide and water (Likáš, et al., 2008; Vieira, et al., 2011).

Lactic and glycolic can be copolymerized by combining them with bioactive ceramics. Poly(lactic-co-glycolic acid) (PLGA) under the trade names Dexon® and Vicryl® have been used as a suture material. For PLGA copolymers a linear relationship between composition, mechanical and degradation characteristics has not been established. The time of degradation depends on the crystallinity of the copolymers (Donglu, 2006).

### **Poly( $\epsilon$ -caprolactone)**

Poly( $\epsilon$ -caprolactone) (PCL) (Figure 4) is a semicrystalline polymer with its low  $T_m$  of 59 °C – 64 °C, low  $T_g$  of about -60 °C. It provides a rubbery consistency at room temperature (Donglu, 2006). As compared with PGA or PLA, PCL degrades significantly slower due its hydrophobic character and crystallinity. PCL is therefore most suitable for the use of long-term implantable system or  $\epsilon$ -caprolactone can be copolymerized with PDLA, PLLA to accelerate the degradation rate (Lanza, et al., 2014).

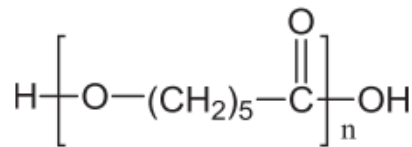


**Figure 4** Chemical structure of PCL (Dimitrios, 2013)

### **Poly(lactide-co-caprolactone)**

The syntheses of poly(lactide-co-caprolactone) (PLCL) (Figure 5) have been widely studied in recent years for potentially improvement properties of PLA and PCL (Yu, et al., 2010). The materials with elastic properties are obtained by copolymerization of lactide and lactone, due to the flexible soft segments which alternate with hard crystalline blocks in the chain microstructure. This also reduces the crystalline features and material degrades faster (Larrañaga, et al., 2014a).

Copolymerization allows choosing wide range properties of the product due to representation of individual groups bringing characteristics features. In addition,

the copolymerization generally decreases concentration of intermolecular bonds as well as the characteristics of values  $T_g$  and  $T_f$  (Jirsák & Kalinová, 2003).

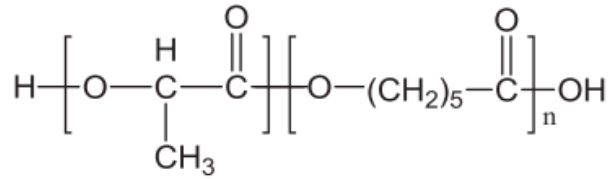


**Figure 5** Chemical structure of PLCL (Dimitrios, 2013)

Fernández et al. (2012a) studied the synthesis, the structure and properties of PLCL copolymers. Their analysis demonstrates a change of properties depending not only on the ratio of L-lactide (LA) and  $\epsilon$ -caprolactone (CL) in the resulting copolymer but also the method and condition of preparation, storage, etc. Results show that the PCL is more stable to thermal degradation than PLLA and their copolymers have intermediate properties of thermal stability. Growing LA content accelerates degradation rate of PLCL due to lower crystallinity and higher water absorption (Grakhal, et al., 2007). The presence of CL units reduces the stiffness and strength. In addition an advantage is minimizing the local acidification and thereby reduced inflammatory response (Vieira, et al., 2011). On the other hand the presence of CL significantly increases the elastomeric character of copolymers, from brittle to ductile behaviour (Fernández, et al., 2012a).

The aforementioned (co)polyesters do not keep the bioactive abilities to induce proliferation and differentiation of cells. But adding some substances e.g. phosphate or silicate based bioactive fillers can improve the bioactivity of polymers in regeneration of soft and hard tissues. Larañaga and et al. (2014a) tested addition of hydroxyapatite and bioglass to PLCL scaffolds. Incorporated bioactive particles reduced elongation at break and tensile strength but also showed excellent adhesion of human adipose-derived stem cells (ADSCs). MTT assays concluded that the studied materials were not cytotoxic for ADSCs.

## **2.3 Production of Polylactide, Polycaprolactone and Their Copolymers**

The traditional ways these polymers may be synthesised are by polycondensation or ring-opening polymerization (ROP), less commonly by enzymatic polymerization (Lopes, et al., 2012). In case of polycondensation, it is difficult to get a high degree of polymerization (high molar mass) and achieve specific groups to provide useful mechanical properties in the final product. Therefore use a two-step synthesizes procedure: hydroxyl acids are transformed into lactones, which are then used in ring-opening polymerizations as monomers (Albertsson, 2002; Donglu, 2006).

### **2.3.1 Polycondensation**

Polycondensation is classical and also economically least demanding production of PLA and PCL, where the input substances are hydroxy acids, and mixtures of diols and diacids or their derivatives. Starting material for the polycondensation reaction generally comes from common chemical synthesis, although some of these can be obtained from renewable resources by fermentation (Albertsson, 2002).

As was mentioned above, the synthesis of polyesters by polycondensation has a large number of weaknesses: not very high proceeds, difficult controllable structure and wide molar mass distribution (high polydispersity index). By this method can be prepared polyester polymers or copolymers up to 45,000 Da, but not in case of pure PLA, where the maximum molar mass is lower, as shown in Nampoothiri work. This process of synthesis requires long reaction times and a precise balance between reactive acid and hydroxyl groups, the reaction takes place at high temperature and by-products are formed (Albertsson, 2002). These must be removed, because they imbalance of reactants or final polymer may contain unreacted chain-extending agents, oligomers and metallic impurities from the catalyst (Ebnesajjad, 2013).

Lactic acid, also known as “milk acid” is an input component for PLA production. It exists in two L and D isomers which normally produce microbial sources. Whereas mammalian produce only L forms, therefore it is better adapted to human metabolism (Ebnesajjad, 2013). The source of acid may be sugar in pure form such as glucose, lactose, etc. or sugar-containing materials such as molasses, potato, wheat, barley, etc.

Acid production by fermentation processes has a positive impact to the environmental friendliness compared to petrochemical resources.

The presence of a hydroxyl (-OH) and a carboxyl group (-C(O)OH) in lactic acid allows it to change directly into polyester. Nampoothiri (2010) indicates that classical polycondensation of lactic acid does not increase the molar mass, hence are used in some acidic catalysts to increase esterification.

PLA can be controllably degrade chemically back to a monomer which can be used again for manufacturing a full-fledged polymer (Petruš, 2011).

Labet (2009) in her work demonstrates the production of PCL by polymerization of 6-hydroxycaproic acid with using catalyst in 2 forms of lipases. The result was polymers with various low molar mass  $5400 \text{ g.mol}^{-1}$  and  $9000 \text{ g.mol}^{-1}$ .

### **2.3.2 Ring-Opening Polymerization**

Ring-opening polymerization (ROP) is a form of chain-growth polymerization. By this process high molar mass (co) polyesters can be prepared to have the desired end groups and advanced macromolecular structures (block, graft and stellate) (Duda & Penczek, 2002). This type of polymerization takes place with a minimum of side reactions under the control of polymer molar mass using the ratio of monomer/catalyst ratio, and to produce products with a low polydispersity index (PDI) (Agarwal, et al., 2002). Besides the initiator character and concentration of catalyst are the main factors affecting the procedure of ring-opening polymerization reaction temperature and time (Albertsson, 2002).

Polymers of lactide and lactones are synthesized exclusively by ROP of their cyclic monomers in the presence of catalyst or initiator. Initiator/catalyst act as a reactive centrum where cyclic monomers respond to open its ring system and form a longer polymer chain. Figure 6 presents the reaction pathway of a cyclic ester by ROP. Each created macromolecule generally contains one chain end of a functional group comes from the termination reaction and one final end capped with a functional group originating from the initiator (Albertsson, 2002).

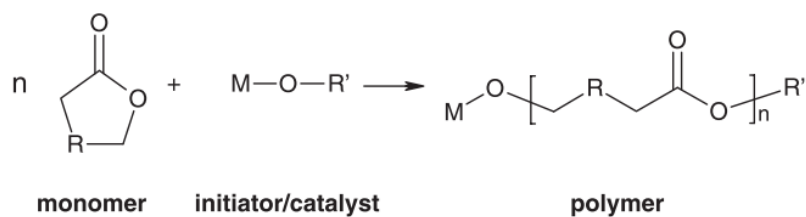


**Figure 6** Schematic representation of the ROP of a cyclic ester  
(Albertsson, 2002)

This type of polymerization is mainly performed in bulk or in solution, but may also be prepared as an emulsion or dispersion reaction. Selection of catalysts, initiators and their functional groups affects the resultant polymer. Depending on the selection of initiator, we distinguish three main reaction mechanisms of polymerization (Albertsson, 2002).

### 2.3.3 Copolymerization

A polymer formed from a mixture of two or more monomers are referred to as a copolymer. The resulting molecules can be characterized by a regular or irregular alternation of monomer units, from blocky to random depending on synthesis conditions, relative rates of incorporation of each monomer (Fernández, et al., 2012a). From two different monomers it is theoretically possible to prepare copolymers with four isomers as shown in Figure 7. PLCL copolymers are most often prepared by ROP with stannous octoate ( $\text{Sn}(\text{oct})_2$ ) as catalyst (Fernández, et al., 2012a; Jiao, et al., 2014; Cohn & Salomon, 2005; Garkhal, et al., 2007). Yu et. al (2010) synthesized PLCL multiblock random copolymer by two-step polymerization method including polycondensation.



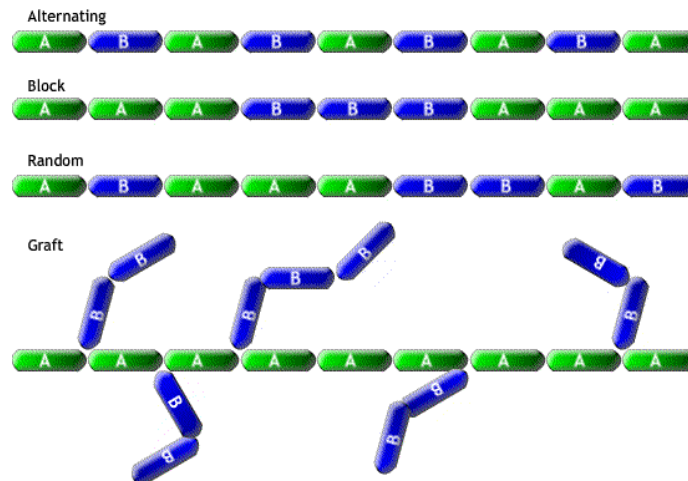


**Figure 7** Illustration of alternating, block, random and graft copolymers  
(University of Cambridge, 2011)

Copolymers with a number of macromolecular architecture and application of units containing a specific functionalized structure give rise to unique properties, e.g. shape-memory behavior, degradation rate, mechanical properties, etc. (Fernández, et al., 2012a).

This does not mean, that the copolymers having similar ratios of monomers will have the same properties. It was found that differences in the chain structure leads to dramatic differences in thermal, mechanical properties, hydrolysis degradation profile and solubility of biopolymers. Degradation process takes place in preference to the amorphous zones than to crystalline parts where degradation rate takes more time. Therefore, random copolymers at equal comonomer ratio are more amorphous than others with higher block unit's distribution. Additionally, random copolymers exhibit the amorphous structure during degradation (Fernández, et al., 2012b).

## 2.4 Biodegradation

Degradation is process leading to a strong change of the material structure by a specific biological activity. The change is characterised e.g. by morphology and topological changes, the formation of degradation products, a strength loss and fragmentation (Tiwari & Srivastava, 2012). Degradation of aliphatic polyesters and others

(polyurethanes, polyphosphorester, and polysaccharides) occurs through scission of the main or side chains of macromolecules. Polymer degradation can be caused by *abiotic factors*, such as light, thermal activation, ultrasonic waves, or *biotic factors* e.g. enzymes, fungi, bacteria and exudates from microorganism (Tiwari & Srivastava, 2012; Nair & Laurencin, 2007).

The cell walls of microorganisms are impassable to macromolecules of polymer. Their input is only possible if bonds of macromolecules are scission into their monomers and oligomers. Enzymes, such as esterase, lipase, protease, etc. produced by microorganisms affect cleaving of large molecules and helps in degeneration of polymer (Tiwari & Srivastava, 2012).

The biodegradation process is usually assumed from measurements of mechanical strength, the molar mass or mass loss due to depletion of low molar mass material (Vieira, et al., 2011) (Lyu & Untereker, 2009). The harmonization of polymer degradation rate with cell seeding and biosynthetic rates characteristics are critical for success of a tissue product (Grakhal, et al., 2007). Biodegradable polymers have to possess:

- Manufacturing practicability, availability of a sufficient quantity of the bulk polymer,
- The ability of the polymer to form the final product design,
- Mechanical characteristics that perform the short-term function (if not intended to fulfil the long-term function),
- Low or insignificant toxicity of products caused by degradation process,
- The capability to be formulated as a drug delivery system in applications with prolonged realise of medicine compounds (Lanza, et al., 2014).

### **2.4.1 Factors Affecting Degradation**

The environmental conditions, such as temperature, pH, humidity, salinity, presence or absence of oxygen and different nutrients, etc. determine the microbial population and the activity of the different microorganisms themselves (Tiwari & Srivastava, 2012; Nampoothiri, et al., 2010). An acidic or alkaline setting can bring different degradation

mechanism and products. For example, polyesters degrade in strong and mild alkalis; PCL is degraded in strong alkalis easily (Tiwari & Srivastava, 2012).

The degradation process is also dependent on the chemical and physical properties of the polymer. These include the chemical morphology and reactivity, structure, molar mass, porosity, crystallinity, cross linking, purity, mechanical strength, etc. There is debate about the influence of the molar mass to the degradation rate. Some authors have suggested that higher activity has the bonds near chain ends which would mean the polymers with lower molar mass can more easily degrade than polymers with higher molar mass themselves (Tiwari & Srivastava, 2012; Nampoothiri, et al., 2010). Others argue that all bonds have identical activity and their degradation mechanism is random (Lyu & Untereker, 2009). Longer chains have more bonds and higher probability of reacting with water.

The storage and the syntheses conditions contribute to the degradation rate. Another aspect to be considered is necessary sterilization before the biomedical material is implanted. Rui and Román (2005) point to sterilization of biodegradable polymers by radiation, which may cause crosslinking or significantly reduce the molar mass of some polymers.

#### **2.4.2 Degradation of aliphatic polyesters**

The aliphatic polyesters have a leading position in families of biodegradable polymers. The major mechanisms for these polymers are *hydrolytic* and *enzymatic degradation*. In hydrolysis, chemical bonds of chains react with water molecules, break up, and produce shorter chains. At the earliest stage the water diffuses into the polymer, the rate of diffusion is controlled by the hydrophilicity/hydrophobicity of the material (Albertsson, 2002). Then primary bonds decompose and it leads to a gradual loss of molar mass and of material. As molar mass decreases, more hydrophilic chain ends are made and samples may absorb increasing amounts of water. The degradation rate is proportional to the concentration of water and hydrolytic polymer bonds (Lyu & Untereker, 2009).

Larrañaga and co-workers (2014b) investigated the degradation of porous and non-porous PLLA, PCL and PLCL scaffolds prepared by solvent casting leaching in phosphate buffered saline (PBS) for a period up to 18 weeks. The results obtained the fastest degradation rate non-porous PLCL with remaining weight 76.6 % then PLLA and the slowest PCL. Porous samples degraded more slowly than non-porous complement because they enable the diffusion of acidic by-products and thus reduce the decline process. This study calculated water absorption ( $WA$ ) and percentage of mass loss ( $WL$ ) according to following equations (1) and (2):

$$WA = \frac{W_w - W_d}{W_d} * 100 \quad [\%] \quad (1)$$

$$WL = \frac{W_0 - W_d}{W_0} * 100 \quad [\%] \quad (2)$$

Samples were removed from the PBS and weighed wet ( $W_w$ ) immediately after the surface wiping. These samples were dried overnight and weighed again to ascertain the dry weight. The abbreviations  $W_0$  and  $W_d$  are the initial and the dry weight of the Sample.

### **Enzyme-catalyzed Degradation**

To accelerate the degradation process in in vitro conditions, it is possible to add a buffer to a small amount of an enzyme. Processes of enzymatic degradation of PLA, PCL and their copolymers have been studied in many publications. However, it is impossible to make any comparison because of different experimental conditions with several of enzymes and their production by different microorganisms.

Zenkiewicz et al. (2013) focused in their study to a comparative analysis of mass losses of PLA, PCL and PHB upon enzymatic degradation. In the test was worked with enzymes – proteinase K, protease, esterase and lipase. Proteinase K caused the highest mass loss. PLA lost after 12 weeks nearly 45 % and PCL of 10 % initial weight. Lipase affected a loss of 4 % in PLA and PCL polymers.

Liu and colleagues (2009) studied enzymatic degradation performed in the presence of proteinase K on various types PLCL copolymers – diblock, triblock and four-armed copolymer with a monomer feed ratio of 50:50. The four-armed copolymer showed

the highest mass loss (30 %) while the diblock copolymer exhibited the smallest loss (10 %). The blocky character supports improvement of the crystallinity due to the less restricted linear structure and bigger strength of bonds.

### **3 Characterization of Polymers**

This discipline deals with the characterization of polymeric materials on different levels. Characterization techniques are typically used for determining the molar mass, molecular structure, morphology, thermal properties and mechanical properties.

Polymers are not as clean as defined by their idealized chemical structure. During the polymerization the polymer may be the polymer polluted by side-reactions, different configuration of monomer units, polymerization conditions, etc. These “contamination” may cause huge differences in physical structure thus causes variations of polymer properties with the same ideal chemical structures (Elias, 2005).

Although there are a number of methods and other tools to study and clarify the structures of macromolecular and low molar mass substances, this work focuses on only two of them, on Gel Permeation Chromatography and Nuclear Magnetic Resonance spectroscopy.

#### **3.1 Determination of Molar Mass Distributions**

Molar mass distribution can be determined by many methods, mainly mass spectroscopy and size-exclusion chromatography (Elias, 2005).

Gel permeation chromatography (GPC), also known as Size-exclusion chromatography (SEC) (Figure 8) is a proven method designed for the samples separation into their constituent parts and procedure for purifying chemicals (Elias, 2005). The basic principle is the distribution of components between mobile and stationary phase. Types of chromatographic methods may be classified according to several aspects. One of them is the types of stationary and liquid phases (liquid, gas), the separation mechanism (adsorption, size exclusion, and ion interaction), method of execution (column, layout area) or even the type of solute (Miller, 2005).



**Figure 8** Gel permeation chromatography analysis system  
(Warwick Scientific Services, 2012)

### 3.1.1 Gel Permeation Chromatography

Gel permeation chromatography (GPC) is the most convenient analytical technique for understanding and predicting polymer performance such as the complete characterization molar mass distribution (MWD) of polymer (Miller, 2005). It separates macromolecules according to their size at a flow rate of the polymer solution of the swollen porous gel in the column, shown in Figure 9. Modern devices allow a wide range of separation from low molar mass to high molar mass within the range of  $10^2$  to  $10^7$  g/mol (Agilent Technologies, 2001).

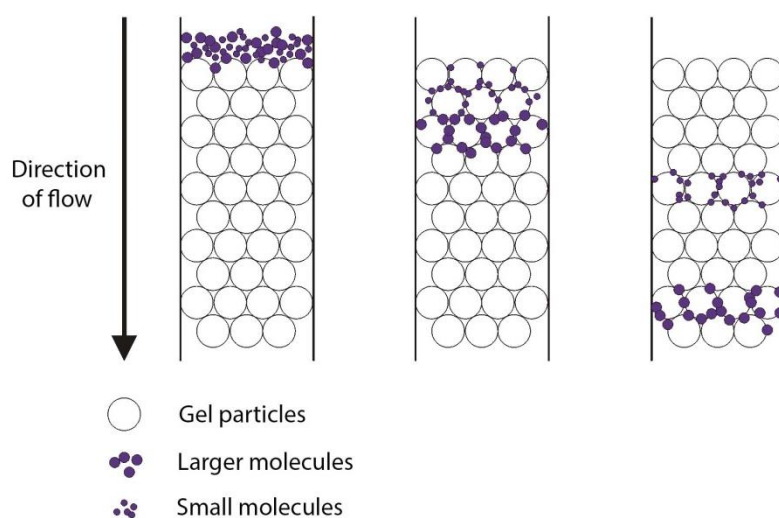


**Figure 9** The size separation mechanism of GPC  
(Waters, 2012)

Molar mass is the most significant structural characteristics of polymers. Subtle differences of values can determine significant variation of the polymer behaviour under different conditions and in the end-use properties. The molar mass and its distribution affect: softening temperature, solubility, viscosity of solution and melts, elasticity, strength, thermal stability, in our case the diameter of the fibre, degradation rate and other properties (especially endurance characteristics) (Waters, 2012; Ducháček, 2006).

The column is filled with small particles of a cross linked gel (e.g. agarose, dextran, poly (styrene)) that contains surface pores of various sizes (stationary phase). The space between the gel and the pores fills a solvent (mobile phase) (Agilent Technologies, 2001). The diluted sample (analyte) injects at the start of the column and it is gradually eluted by a mobile phase. The smallest molecules of sample can diffuse into the interior of the gel and are longest retained in the column while the middle molecules get only into the larger pores. Molecules larger than the pores of the gel pass the column without detention, so they have the smallest retention time (Waters, 2012).



The concentration of the exiting solution is measured as function of time or eluent volume, via concentration-sensitive detectors refractive index (RI) or ultraviolet (UV) photometer (Elias, 2005).

The gel permeation chromatograph contains a number of different components:

- pump – ensuring a constant flow of solvent in system,
- injector – the sample introduces into the mobile phase,
- column set – separation of the individual sample components,
- detector(s) – monitoring of separation,
- data processing equipment - calculations and report of the molar mass averages and MWD (Waters, 2012).

Scheme of a basic GPC device is shown below in Figure 10.

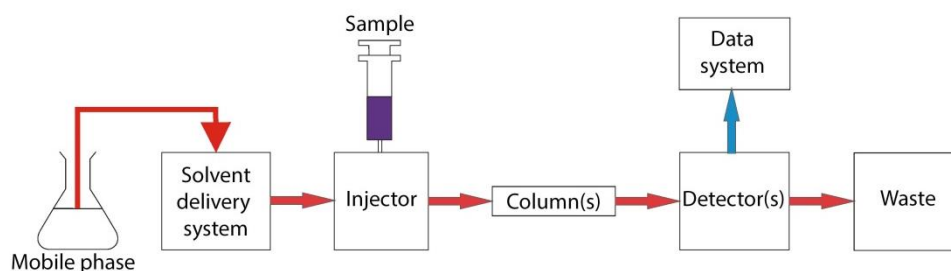


**Figure 10** Scheme of GPC device  
(Waters, 2012)

The main disadvantage of this method is filtration of the samples before the actual measurement and limited number of peaks caused by the short time run of GPC. Due to filtration may be removed higher molar mass sample before it can be loaded on the column (Elias, 2005).

## 3.2 Nuclear Magnetic Resonance Spectroscopy

Abbreviation NMR means Nuclear Magnetic Resonance. NMR, shown in Figure 11, is used to study structure of molecules, the interaction and the composition of mixtures of synthetic or biological solutions or compounds (Bruker, 2014). This analytical

method works on the interaction of an oscillating radio-frequency electromagnetic field with a set of nucleus inserted into a strong external magnetic field (Macomber, 1998).



**Figure 11** NMR Spectroscopy Analyser (Azom, 2011)

NMR deals with the matters of atomic nuclei in a magnetic field. In the simplest description, the atomic nucleus contains two particles – positively charged proton and electrically neutral neutron. Each of these particles has important property called *spin*. Simply we can say that is the direction of the rotary motion of the particle. The spin characteristic tells us if that nucleus is suitable for NMR spectroscopy or not. The nuclei with a zero value are nonmagnetic and these cannot be detected by NMR. The most commonly studied nuclei are  $^1\text{H}$  and  $^{13}\text{C}$  (NMR laboratoř PřF MU, 2014).

Without a magnetic field, the spins have the same energy which means that are randomly arranged. If an external magnetic field is activated, spins will divide into two levels. One will have less energy compared to the basic state, the second contrarily higher. These levels are irradiated by radiofrequency radiation. After completion of the irradiation excited atom converts in the ground state (deexcitation) which is measured (NMR laboratoř PřF MU, 2014).

The NMR spectrum includes signals known as *peaks*, which are characterized primarily by chemical shift ( $\delta$ ) and intensity. The intensity of the signal corresponds to the quantity of the spin system and the chemical shift is the chemical surroundings of the measured nucleus. Nucleus is part of the molecule that surrounds bonding

electrons. They behave as small local magnets and have an impact to the intensity of the external field these nuclei. Hence a resonant frequency of nuclei dependent on chemical surroundings of the measured nucleus (NMR laboratoř PřF MU, 2014).

## **4 Electrospinning**

One of the main issues of the work is the optimization and production of nanofibre layer using Nanospider TM machine. This chapter explains the basic principle of fibre production by electrospinning and its process parameters that influence the final fibres.

Electrospinning has a number of techniques how nano/microscale fibres can be processed through an electrically charged jet of polymer solution or melt (He, et al., 2008). The simplest form of electrospinning process consist direct current (DC) power supplier with a range of kilovolts (kV) and two electrodes: a capillary (a rod) to hold polymer solution and collector for collecting fibres (Ramakrishna, et al., 2005). An electric field is generated between the capillary and the metallic collector induces charging of the polymer droplet on the capillary held its surface tension. At the critical voltage the reciprocal attraction between the charged droplet surface and the collector cause an elongation to form a conical shape known as the Taylor cone (Stanger, et al., 2005). At the exceeding this critical voltage the repulsion of the electrostatic force overcome the surface tension, a jet on the tip of Taylor cone ejects toward the collector in a random manner. During acceleration a solvent evaporates, in case of polymer solution, the jet is rapidly thinned and lengthened (He, et al., 2008).

A modification of capillary/ needle may allow the production of fibres with unique structures and properties, therefore several variations of electrospinning have been investigated. These variations come in the form, e.g. a rod (instead of needle), two coaxial needless or the form of needless electrospinning (Ramakrishna, et al., 2005).

### **4.1 Electrospinning Process Parameters**

The diameter of the nanofibres is a key parameter for most of the applications. It controls structural characteristics such as pore sizes and specific areas in nonwovens which affect the cell proliferation in TE or the capability and the permeability of filters (Wendorff, et al., 2012). The final properties of electrospun fibres influence numerous parameters. These factors can be divided into three broad categories:

- Properties of solution and feedstock (solution parameters)
- Design, geometry of the electrospun supply (processing parameters)
- Atmospheric and other local conditions (environmental parameters), Table 2 (Mitpuppatham, et al., 2004).

**Table 2** *Electrospinning process parameters* (Mitpuppatham, et al., 2004)

<b>Polymer solution parameters</b>	<b>Processing parameters</b>	<b>Environmental parameters</b>
Concentration	Electrostatic potential	Temperature
Viscosity	Electric Field Strength	Humidity
Surface Tension	Electrostatic Field Shape	Local Atmosphere Flow
Conductivity	Working Distance	Atmospheric composition
Permittivity	Feed Rate	Pressure
Solvent Volatility	Orifice Diameter	

#### **4.1.1 Polymer Solution Parameters**

The properties of the polymer solution have the most significant influence for final fibre morphology. Polymers with higher molar mass dissolved in a solvent will have higher viscosity than solution of the same polymer with lower molar mass (Wendorff, et al., 2012). The molar mass represents the length of the chain and it will determine the quantity of entanglement in the solvent. The fibre diameter grows with the increasing concentration of the solution. The viscosity is connected with surface tension. In case of higher concentration of free solvent molecules is a greater tendency to accumulate in a spherical shape leading to the beads formation because a liquid surface is trying to achieve a state with the lowest energy. To reduce the surface tension, use a solvent which has a low surface tension or add surfactant to the solution. It was found that both methods lead to yield more uniform fibres (Ramakrishna, et al., 2005).

Use of solvent with a very low volatility causes storage of a wet fibre mat or a film with pores on the collector. However, if the solvent is too volatile the Taylor cone becomes stiff, that halts fibre production (Stanger, et al., 2005).

### **4.1.2 Processing Parameters**

The usual strength of the electric field to start electrospinning is around 0.5 and 1.5 kV/cm, the work by Taylor demonstrates a minimum voltage as 6 kV (Stanger, et al., 2005). This is only an approximate value, because the greatest influence has viscosity and the type of the spun solution. A higher voltage causes faster acceleration of the jet and more volume of the solution will be drawn from the needle. An inadequate feeding rate causes a smaller and less stable Taylor cone. Possibly the Taylor cone may recede into the needle. It was found that a higher voltage growth has a tendency for beads formation (Ramakrishna, et al., 2005).

A larger distance between the tip of the needle and the collector (working distance) prolongs the flight time of the electrospinning jet, which may favour the formation of finer fibres. (Ramakrishna, et al., 2005). In other cases, the bigger distance has results thicker fibres due to a reduction of the electric field (Stanger, et al., 2005).

### **4.1.3 Environmental Parameters**

The success of the electrospinning of some polymers depends on the humidity and the temperature. Some hydrophobic materials require less humidity than others and conversely. The amount of humidity affects not only a formation of pores but also the rate of evaporation of the solvent in the solution. The size and the depth of pores increase with increasing humidity. Conversely at a low humidity, a volatile solvent can evaporate rapidly and may block the needle (Ramakrishna, et al., 2005).

## 5 Experimental Part

Aim of the experiment was to optimize the electrostatic spinning process for copolymers PLCL and the creation of nanofibre layers by the Nanospider TM machine produced by Elmarco. Default copolymers differed from each other in several features – the ratio content of lactide:lactone, molar mass, different chain microstructures, etc.

The biodegradation of the fibrous layers of the copolymer has been mainly investigated. For this purpose, the enzyme-catalyzed degradation tests with proteinase K were performed. The result was the mass decrease of material and the associated changes in molar mass measured by gel permeation chromatography. Degradation of the copolymers was also confirmed by morphological changes of the fibers. All the results were processed and evaluated. At the end of the experimental work is mentioned discussion and conclusion.

### 5.1 Characteristics of Polyester Copolymers

Several materials have been used in this work. One of them is a commercial product PURASORB PLC (hereafter referred under the name PLCL\_p) obtained from PURAC Biochem (The Netherland). Other two PLCL materials with catalogue number AP74 and AP067 (hereafter referred under the name PLCL\_pls and P(L)CL\_pls are from PolySciTech (Akina, USA). Last three copolymers were synthesized at Chiang Mai University in Thailand for the purpose of this work (hereafter referred under the name of PLCL\_th\_1, PLCL\_th\_2 and PLCL\_th\_3).

Date sheets of commercial products are mentioned in Appendix 1.

#### 5.1.1 Detection of Molar mass by GPC

The molar mass of copolymer including number average molar mass ( $M_n$ ), the weight average molar mass ( $M_w$ ) and polydispersity index ( $PDI = M_w/M_n$ ) were determinate by gel permeation chromatography (GPC).

The measurements were performed with Agilent 1100 Series HPLC Value System with an ultraviolet (UV) and a refractive index (RI) detectors. The GPC system was operated at 40°C and was composed of two polyester (PL) gel mixed-B columns 10 µm 300 x 7.5 mm and one mixed-C column 5 µm 300 x 7.5 mm. The columns were calibrated with narrow EasiVial Polystyrene PS-M Standards (Agilent). All data were analysed by software package supplied by Agilent Technologies. Tetrahydrofuran (THF) (>99.5 %, Fisher Chemical) containing 2% (v/v) triethylamine (TEA, ≥99 %) provided by Sigma Aldrich was used as the eluent at a flow rate of 1.0 ml/min.

It is important to think about the injection volume and polymer concentration in mobile phase during the sample preparation procedure, as they affect the peak position and its shape. The optimal concentration and injection quantity depends on the molar mass of analysed material. Materials with higher molar mass have a higher viscosity which may slow down the diffusion process inside the GPC columns. The retention time will increase as a consequence of deceleration and the calculation of molar mass leads to lower value (Fernández, et al., 2012a). Similar concentrations and uniform injection volume 1.0 ml/min were kept.

Each sample of copolymer was dissolved in the mobile phase of 1 ml volume, which additionally contained 0.4 v/v % of toluene (98.9 %, Fisher Chemical). The dissolution took place at the room temperature using mechanical stirring. To remove impurities, all samples were filtered with non-sterile 4 mm syringe filter units (Millex®, Millipore) with pore size 0.45 µm and hydrophilic poly(tetrafluoroethylene) (PTFE) membrane.

The GPC analyses of all copolymers are mentioned in Table 3, showed the number average molar mass ( $M_n$ ), the weight average molar mass ( $M_w$ ) and the polydispersity index (PDI). The polydispersity index ranged from 1.62 to 2.03.

**Table 3** Molar masses of copolymer granules

Sample name	Refractive index detector		
	$M_w$ [g/mol]	$M_n$ [g/mol]	PDI [-]
PLCL_p	193,000	94,900	2.03
PLCL_th_1	93,500	48,900	1.91
PLCL_th_2	122,900	69,800	1.76
PLCL_th_3	54,000	30,000	1.78
PLCL_pls	90,800	47,900	1.90
P(L)CL_pls	77,000	47,400	1.62



GPC data were obtained by measurement of refractive index (RI), and are presented in Figure 9. Additional GPC data obtained via UV absorbance are presented in Appendix 2.

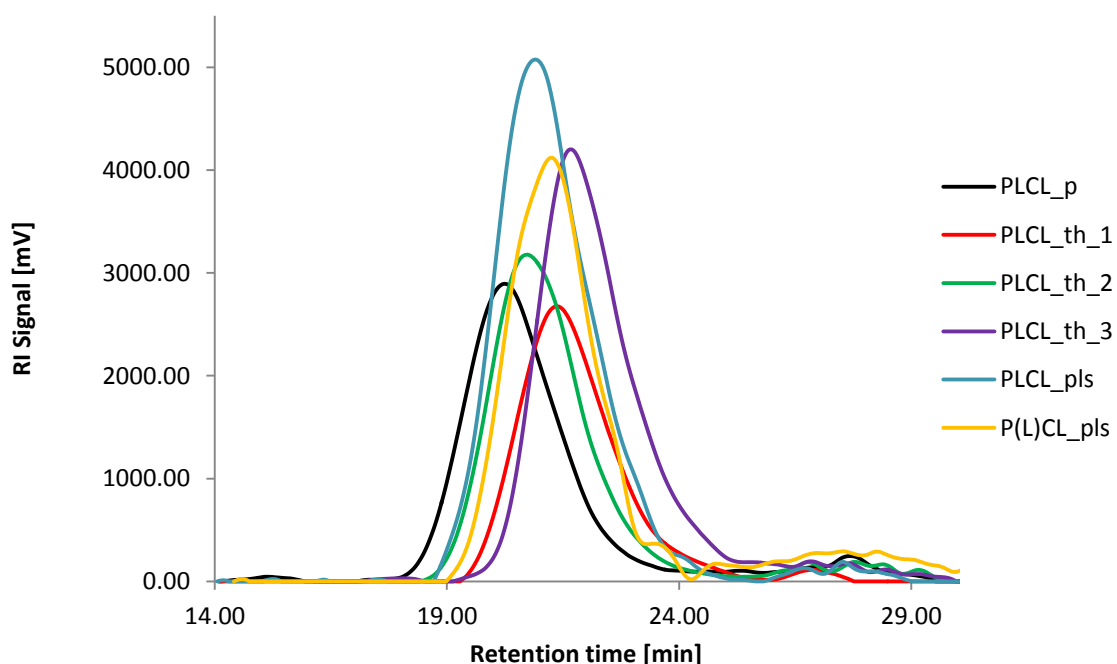


**Figure 12** Molar mass distribution of PLCL copolymers

Figure 12 shows the molar mass distribution (MWD) of PLCL copolymers. A single peak of all samples indicates the successful copolymerization. Copolymer P(L)CL\_pls (Figure 12, yellow peak) shows the second smallest peak at 24 min. This peak may represent shorter polymer chains (e.g. unreacted) or any contamination caused by synthesis process (e.g. initiator, catalyst).

The graph demonstrates that the copolymer PLCL\_p has the shortest retention time and therefore the highest number average molar mass 94,900 g/mol. The second highest molar mass was demonstrated by PLCL\_th\_2 (69,800 g/mol), followed by PLCL\_th\_1 (48,900 g/mol) with very similar outcomes as PLCL\_pls (47,900 g/mol) and P(L)CL\_pls (47,400 g/mol), and the copolymer PLCL\_th\_3 had the lowest  $M_n$  (30,000 g/mol).

Although various molar mass are reported by manufacturers is not possible to compare them with each other due to the different calibration standards, used columns, mobile phases, etc. The measurements were therefore made for all samples under the same conditions. Data sheets from manufacturers of individual products are listed in Appendix 1.

### 5.1.2 $^1\text{H}$ NMR Characterization

The copolymer composition and chain microstructure of PLCLs were examined by hydrogen-1 nuclear magnetic resonance spectroscopy ( $^1\text{H}$  NMR). Proton spectra were obtained on a Bruker Avance at 300 MHz. Deuterated chloroform ( $\text{CDCl}_3$ ) (99.8%, Cambridge Isotope Laboratories Inc., USA) with 0.05 v/v % tetramethylsilane (TMS) was used as a solvent. TMS gives a zero frequency reference for NMR spectra. Chemical shifts are given in parts per million (ppm).

The amount of 5 – 8 mg of polymer sample was dissolved in ca. 1 ml of a deuterated solvent, filtered, and placed in 5 mm glass NMR tube. Samples were filtered otherwise it could adversely affect the resolution and line shape. Without filtration the resolution and line shape could be adversely affected.

#### Calculation of Molar Ratio LA:LC

The percentages of lactide and lactone monomers incorporated into polymer chains were calculated from the  $^1\text{H}$  NMR integral area (labelled as  $S_{\text{PLA-CH}}$  and  $S_{\text{PCL-CH}_2}$ ). The analysis of the spectrum was performed using works by Peponi and et al. (2012) as references. The methylene signal of polycaprolactone ( $-\text{CH}_2-$ ) is detected around  $\delta = 4.00$  ppm, and the multiplet of polylactide ( $-\text{CH}-$ ) occurs around  $\delta = 5.05 - 5.20$  ppm with some unpolymerized lactide at approximately  $\delta = 5.03$  ppm. The resonance at  $\delta = 0$  ppm is assigned to TMS,  $\delta = 1.3 - 1.7$  are assigned to lactone ( $-\text{CH}_2)_3-$  and lactide ( $-\text{CH}_3$ ), and  $\delta = 7.26$  ppm is  $\text{CDCl}_3$ . Figure 13 shows the  $^1\text{H}$  NMR spectrum of PLCL\_th\_1. The picture also indicates the chemical structure of copolymer PLCL, positions of hydrogens in the chain and their corresponding resonances in the spectrum.

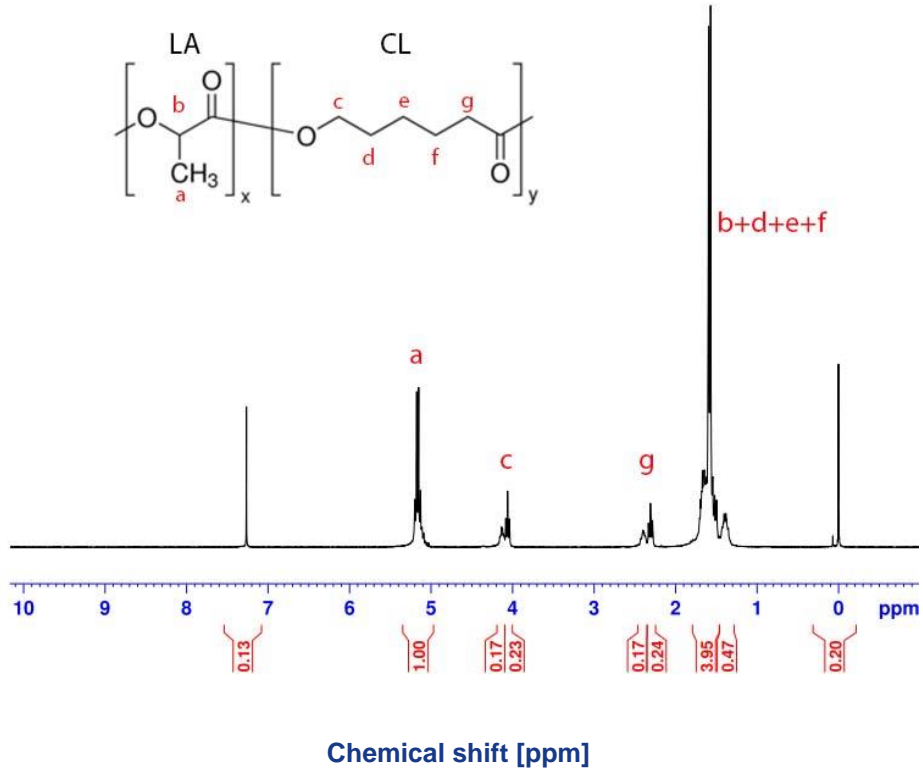


**Figure 13**  $^1\text{H}$  NMR spectrum of PLCL\_th\_1

The integrals for  $\text{CH}_2$  (at 1.4 ppm) and  $\text{CH}$  (at 5.2 ppm) are attributed to PCL ( $S_{\text{PCL-CH}_2}$ ) and PLA ( $S_{\text{PLA-CH}}$ ) respectively. Therefore, for PLCL\_th\_1  $S_{\text{PCL-CH}_2} = 0.40$  and  $S_{\text{PLA-CH}} = 1$  as shown in Figure 13 above. The percentages of chains composition lactide (LA) and lactone (LC) in PLCLs copolymers was obtained from the following equation (3) and (4):

$$LA = \frac{S_{\text{PLA-CH}}}{S_{\text{PLA-CH}} + \frac{S_{\text{PCL-CH}_2}}{2}} * 100 \quad [\%] \quad (3)$$

$$LC = \frac{\frac{S_{\text{PCL-CH}_2}}{2}}{S_{\text{PLA-CH}} + \frac{S_{\text{PCL-CH}_2}}{2}} * 100 \quad [\%] \quad (4)$$

The percentage ratios of lactide and lactone detected in all PLCL copolymers are set out in the table below. Table 4 shows the relative integrals of each resonance. The  $^1\text{H}$  NMR spectra of the all copolymers are listed in Appendix 3.

**Table 4** Molar ratio of LA:LC detected by <sup>1</sup>H NMR

Sample name	Molar ratio of LA:LC [%]		Integral area	
	LA	CL	S <sub>P<sub>LA</sub>-CH</sub>	S <sub>P<sub>CL</sub>-CH<sub>2</sub></sub>
PLCL_p	82	18	1	0.43
PLCL_th_1	83	17	1	0.40
PLCL_th_2	67	33	1	0.98
PLCL_th_3	40	60	1	3.04
PLCL_pls	60	40	1	1.34
P(L)CL_pls	39	61	1	3.13

### Copolymers Chain Microstructure

One of the properties that have a significant impact on the degradation profile is the chain microstructure. Therefore, <sup>1</sup>H NMR spectroscopy was used to probe the distribution of LA and LC units in the copolymers. For this calculation, integral areas of two resonances from spectra at  $\delta = 2.30$  ( $S_{CL-CL}$ ) and  $\delta = 2.50$  ppm ( $S_{CL-LA}$ ) are necessary. The first resonance at  $\delta = 2.30$  ppm represents CLCL (-CH<sub>2</sub>COOCH<sub>2</sub>-) junctions and the second resonance at  $\delta = 2.50$  ppm indicates CLLA (-CH<sub>2</sub>COOCH-) junctions (Darensbourg, 2010). The proportions of CLLA and CLCL junctions were obtained by equations (5) and (6):

$$CLLA = \frac{S_{CLLA}}{S_{CLCL} + S_{CLLA}} * 100 \quad [\%] \quad (5)$$

$$CLCL = \frac{S_{CLCL}}{S_{CLCL} + S_{CLLA}} * 100 \quad [\%] \quad (6)$$

Table 5 presents the proportions of alternating monomer units (CLLA), and non-alternating monomer units (CLCL) in individual copolymer chains. It shows that different chain structures vary from random to blocky character.

**Table 5** Chain microstructure - monomer alternation

Sample name	Monomer alternation [%]		Integral area	
	CLLA	CLCL	S <sub>CLLA</sub>	S <sub>CLCL</sub>
PLCL_p	67	33	0.28	0.14
PLCL_th_1	41	59	0.17	0.24
PLCL_th_2	37	63	0.36	0.62
PLCL_th_3	24	76	0.74	2.34
PLCL_pls	40	60	0.58	0.87
P(L)CL_pls	25	75	0.79	2.57

Although PLCL\_p and PLCL\_th\_1 have very similar composition with regard to the ratio of LA:CL, 82:18 and 83:17, the chain structures are completely different. PLCL\_p has random character because it presents a higher content of CLLA junctions which is 67%. On the contrary PLCL\_th\_1, and other copolymers, display block copolymer character, where content of CLLA is less than 41 %.

### **5.1.3 Electrospinning Process Optimization**

As previously mentioned in the introduction to the experimental part, one of the objectives of this work is the creation of fibre layers from the PLCL copolymers. The aim of this chapter is to find the optimal solution concentrations, suitable solvent and optimal electrospinning conditions.

All copolymers were dissolved in a solvent mixture of chloroform:ethanol:acetic acid in the ratio 8:1:1 (w:w:w) to concentration between 5 and 20 w/w % . The optimization took place on the needle electrospinning device with the blunt-ended needle dosing at the flow rate of 2 ml/h, a voltage of 15 kV, with distance between the metal collector and needle tip of 20 – 30 cm and 30 – 40 % relative humidity at the room temperature. The copolymers were spun on to paper or aluminium foil during the optimization. Microscopic structure was investigated by scanning electron microscopy. A complete overview of SEM images of PLCL\_th\_1, PLCL\_th\_2 and PLCL\_th\_3 with average fibre diameters and histograms are presented in Appendix 4.

Subsequently the concentration for each copolymer was selected and spun on the Nanospider TM machine produced by Elmarco. PLCL\_p copolymer was spun with a concentration of 8 w/w % and PLCL\_th\_1 at the concentration of 14 w/w %, in chloroform:ethanol:acetic acid (8:1:1, w:w:w). Table 6 lists the process conditions at which the nanofibre layers were prepared.

**Table 6** Nanospider TM process conditions

Process conditions	PLCL_p	PLCL_th_1
+ Electrostatic potential [kV]	35	35
- Electrostatic potential [kV]	10	15
Rewinding speed [mm/min]	15	20
Rotation/wire speed	45	58
EMW speed [mm/sec]	320	325
Electrode distance [mm]	194	206
Temperature [°C]	24.4	24.6
Humidity [%]	15.3	14.6

Other copolymers PLCL\_th\_2, PLCL\_th\_3, PLCL\_pls and P(L)CL\_pls could not be optimized for fibres formation. Several techniques and experiments were carried out to obtain fibres. The only foils and fused meshes were prepared instead.

This phenomenon may be caused by a higher proportion of lactone in the copolymers. Kwon and colleagues (2005) reported the influence of the ratio of lactide:lactone on the mechanical properties of fibres prepared by electrospinning. Copolymers with increasing ratio of lactone exhibited an inherent physical property of a gum-like state. Fibres with lactide:lactone in a ratio of 50:50 were highly elastomeric and showed a low Young's modulus and an almost linear stress – strain relationship. They were unable to successfully spin their copolymer with LA and CL the ratio of 30:70, and only produced fused meshes, like those reported in this work.

#### **5.1.4 Surface Morphology Observed by SEM**

It was necessary to probe the structures of the fibres by visual evaluation. Accordingly, the surface morphology of fibre layers of copolymers PLCL\_p and PLCL\_th\_1 (Figure 14) were evaluated by scanning electron microscopy (SEM).

Samples were coated with 5 nm layer of gold with a Quantum Q150R – ES, and SEM images were acquired on a Vega Tescan TS 5130.

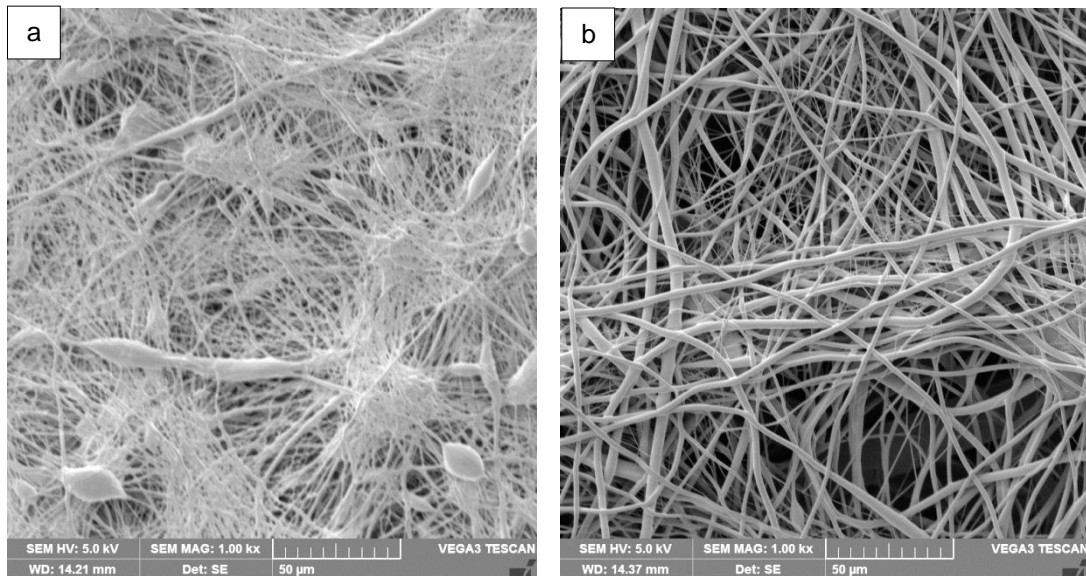


**Figure 14** SEM images of fibres structure of a) PLCL\_p, b) PLCL\_th\_1, magnification 1000x, scale 50  $\mu\text{m}$

Next, the images were analysed to determine the structural parameters for each fibre layer. The average fibre diameter (the measurement of 100 fibres) was evaluated with ImageJ software. The projected area diameter of the inter-fibrous area was obtained by using NIS Elements AR 3.0 software. For all measurements, 1000 times magnified images were used. The observed fibre diameter of PLCL\_p is  $0.58 (\pm 0.22) \mu\text{m}$  and  $1.62 (\pm 0.97) \mu\text{m}$  for PLCL\_th\_1. The average inter-fibrous area was estimated to  $2.1 (\pm 1.24) \mu\text{m}$  for PLCL\_p and  $3.28 (\pm 2.08) \mu\text{m}$  for PLCL\_th\_1. Figure 15 and 16 provides illustration of a measured fibre diameter distribution of PLCL\_p and PLCL\_th\_1 fibrous layers. Table of measured data are listed in the Appendix 5.

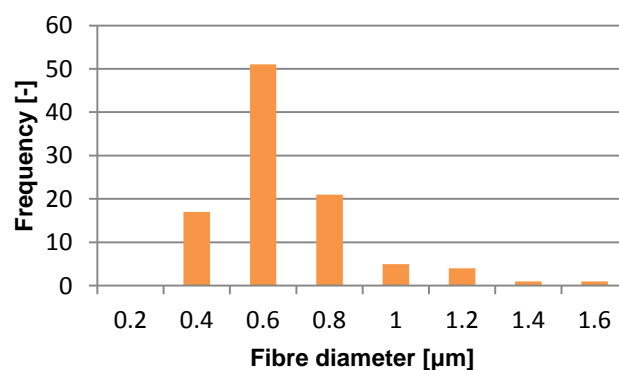


**Figure 15** Histogram of PLCL\_p

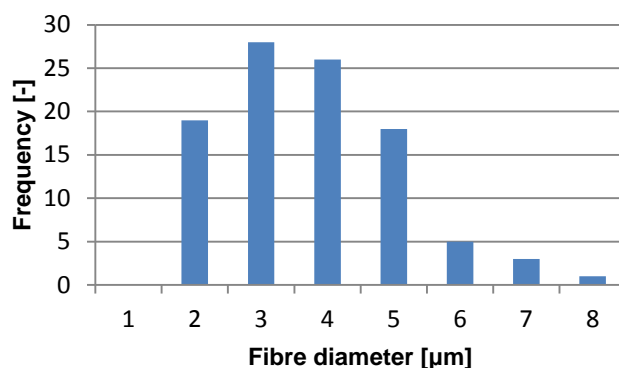


**Figure 16** Histogram of PLCL\_th\_1

## 5.2 Proteinase K-catalyzed Enzymatic Degradation

Nanofibrous layers of copolymer PLCL\_p and PLCL\_th\_1 were both subjected to degradation experiments (samples electrospun on Nanospider TM, for conditions see Chapter 5.1.4).

After the degradation experiments, the test process was optimized and the number of units of proteinase K required for the main experiment was determined.

### 5.2.1 Materials and Methods

According to the literature, proteinase K is the most successful enzyme for the degradation of aliphatic polyesters, and so was chosen for use in the degradation experiments. The enzyme proteinase K (from *Tritirachium album*) as a powder was supplied by Sigma-Aldrich (USA) with a specific activity of  $\geq 30$  units/mg (U/mg). Maximum enzyme activity obtained at 37 °C with pH = 7.5 to 9.0 (Sigma-Aldrich, 2014).

Samples of 50 mg mass (without supporting spunbond fabric) were cut out from the flat fibre layer of size about 40 mm x 30 - 50 mm. As the thickness of the layers PLCL\_p and PLCL\_th\_1 were different, a uniform mass of the samples was kept. Weights of samples diverged by a maximum value of 4 mg. Table with weights of all samples is given in Appendix 6.



## 5.2.2 Amount Optimization of Enzyme

The hydrolytic/enzymatic degradation study was investigated in 0.1 M Tris buffer medium with pH = 8 (The composition of 0.1 M Tris buffer is specified in Appendix 7), containing 0.02 v/v % of sodium azide ( $\text{Na}_3\text{N}$ ) and 10 U/ml or 20 U/ml of proteinase K. The studied copolymer samples were placed in 15 ml Falcon tubes with 5 ml of Tris buffer solution and kept at a constant temperature of 37 °C. The Tris buffer with enzyme was removed by centrifugation (on Hermle Z 36 HK at speed 4,500 rpm) and decantation, and then replaced, every 24 hours, for 3 days. After two days, the materials began to disintegrate and no longer held the original shape of fibre layer.

### Mass Loss

Each sample was taken directly from the buffer and transferred onto previously weighed filter paper (5.5 cm diameter, No. 389 FILTRAK), washed carefully three times with distilled water and placed on to a piece of parafilm. This was followed by drying for 3 days at 37 °C. The mass loss was measured after 24, 48 and 72 hours. The samples were weighed with a digital balance (max = 120g, Atilon) with an accuracy of  $\pm 0.1$  mg. The percentage of mass loss ( $Wl$ ) was calculated according equation (1) described in the Chapter 2.4.2.

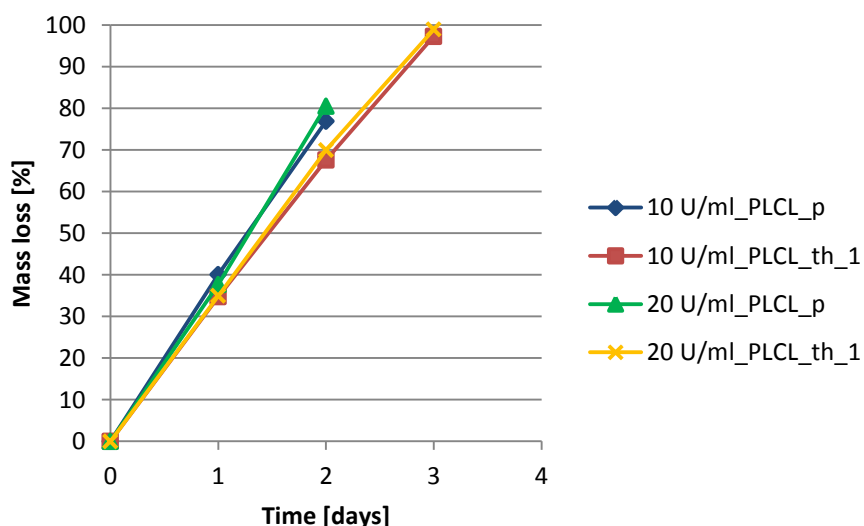


**Figure 17** Mass loss of PLCL with 10 U/ml and 20 U/m of enzyme

Figure 17 shows the mass loss profiles of the copolymers used in this study with the different amounts of enzyme. Mass loss was in two first days faster in case of PLCL\_p. After two days PLCL\_p lost 77 % (10 U/ml) and 80 % (20 U/ml) of its initial weight. By day three PLCL\_th\_1 with 10 U/ml of proteinase K had lost 97 % of its initial mass, and PLCL\_th\_1 with 20 U/ml of enzyme had lost 98 %. Values of mass loss were obtained from measurements of one sample.

After two days of application of the enzyme the material PLCL\_p completely lost its fibre character. The material was disintegrated into small pieces, thereby was confirmed as a suitable choice of the enzyme and the test was stopped. PLCL\_th\_1 layer still hold its external appearance after two days. Therefore it could not be clearly defined if the enzyme worked for this material or not. For this reason the test continued until the third day when the material began to crumble as PLCL\_p.

### Molar Mass Change

Further changes in molar mass were measured after the first and second day in a buffer with 10 U/ml and 20 U/ml of proteinase K. After the third day the material lost significant mass and therefore it was not detectable for GPC analysis.

A complete overview of the molar mass of the experiment is placed in Table 8 below.

**Table 7** Molar mass loss with 10 U/ml and 20 U/ml of enzyme

10 U/ml of enzyme				
Time [days]	PLCL_p		PLCL_th_1	
	M <sub>n</sub> [g/mol]	PDI [-]	M <sub>n</sub> [g/mol]	PDI [-]
0	73,600	1.81	35,100	1.70
1	42,100	3.37	23,300	2.01
2	34,100	3.414	4,500	1.15
20 U/ml of enzyme				
Time [days]	PLCL_p		PLCL_th_1	
	M <sub>n</sub> [g/mol]	PDI [-]	M <sub>n</sub> [g/mol]	PDI [-]
0	73,600	1.81	35,100	1.70
1	45,800	2.24	23,100	2.06
2	34,500	3.46	14,100	3.38

The solvent system used for the electrospinning contained acetic acid which leads to the chain scission (Vieira, et al., 2011). It was not sufficient to only measure the molar mass of the initial copolymer in the granular form; therefore it was necessary to determine the molar mass of the spun fibrous structures. The spun copolymers showed a molar mass loss of 4 % for PLCL\_th\_1 and 13 % for PLCL\_p. These values (labeled as 0 day) were the default numbers for the detection of molar mass loss. Changes in molar mass of PLCL\_p and PLCL\_th\_1 after application of enzyme are shown in Figure 18.

For the copolymer PLCL\_p the concentration of enzyme did not have a significant influence. In both cases molar mass decreased more than 50 %. On the other hand, the molar mass of PLCL\_th\_1 changed substantially depending on the quantity of enzyme. PLCL\_th\_1 with concentration of 10 U/ml and 20 U/ml lost 34 % and 60 % of the initial molar mass; PLCL\_p lost 54 % and 60 %.

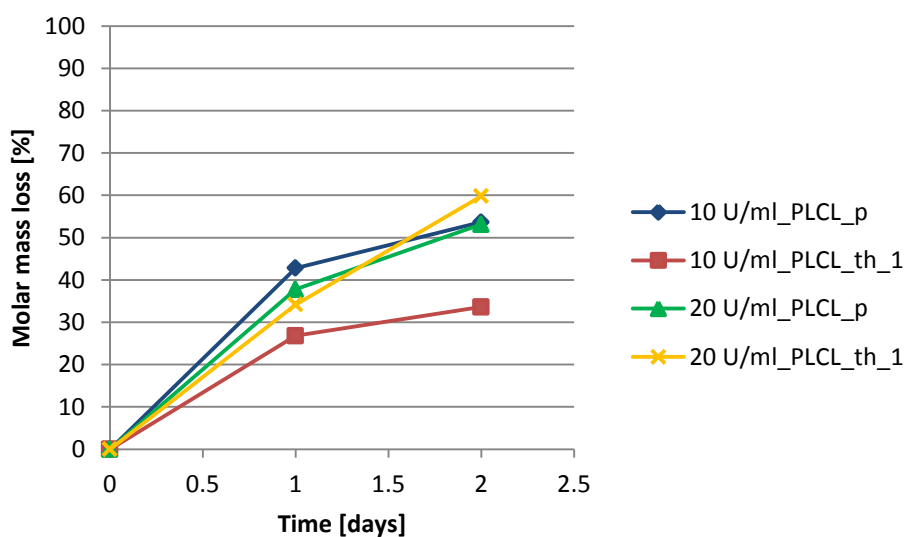


**Figure 18** Molar mass loss with 10 U/ml and 20 U/ml of enzyme

During the samples preparation for GPC analysis the interesting phenomenon was occurred. It was not possible to completely dissolve the samples from the first day. As it is necessary to filter the sample before the analysis, it is possible that the larger molecules did not pass the filter and thereby the molar mass can be influenced.

## Surface Morphology Change during Degradation

It was necessary to image the fibre structures to perform image analysis and visual evaluation. The surface morphology of degraded fibrous layers of both copolymers PLCL\_p (Figure 19) and PLCL\_th\_1 (Figure 20) were evaluated by scanning electron microscopy (SEM) by Vega Tescan TS 5130.

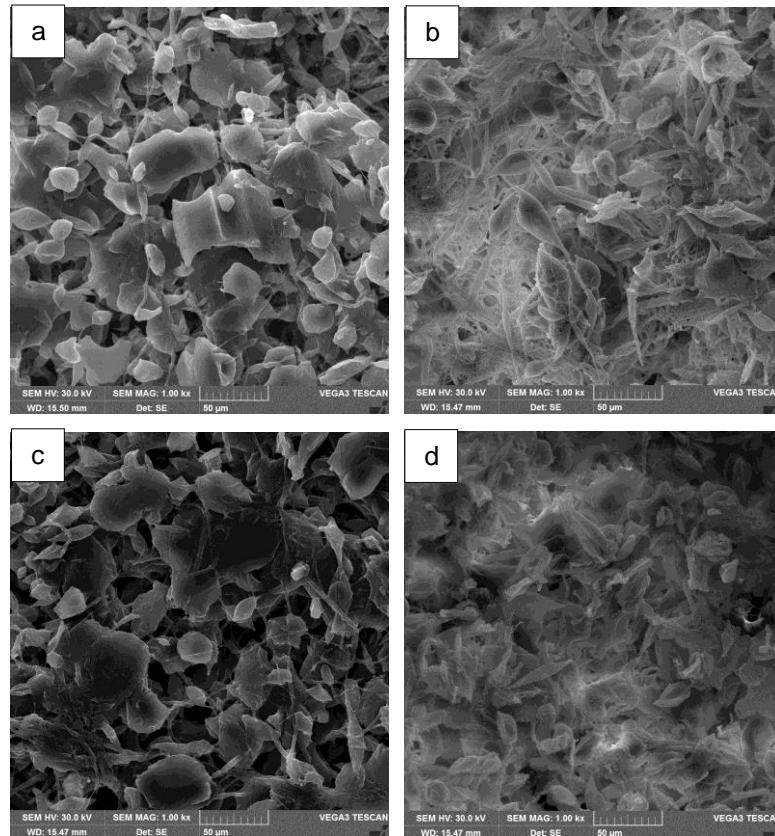


**Figure 19** SEM images of PLCL\_p with 10 U/ml (a, b) and 20 U/ml (c, d) of enzyme after 1 day and 2 day of degradation, magnification 1000x, scale 50 µm

After the first day of degradation PLCL\_P occurred to lose the fibrous nature of the material. Most of the fibres disintegrated and formed to lumps. On the morphology change did not have an application amount of 10 U/ml or 20 U/ml of enzyme any difference.

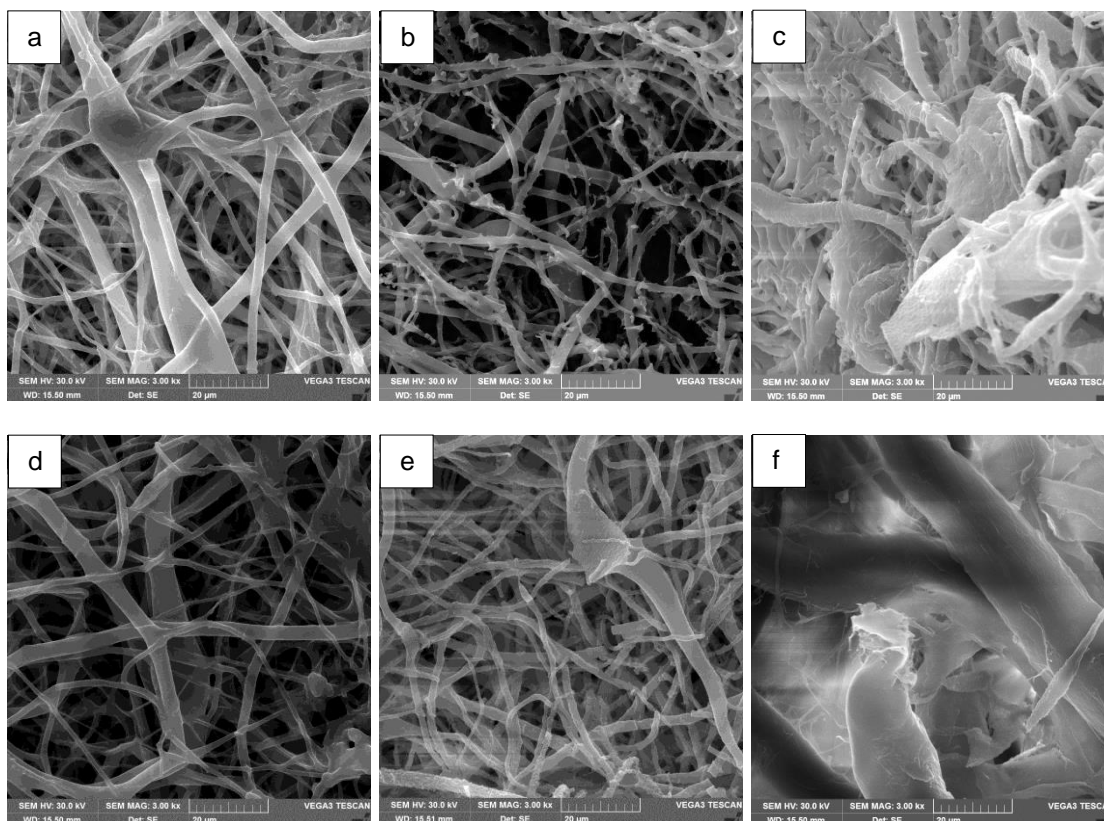


**Figure 20** SEM images of PLCL\_th\_1 with 10 U/ml (a, b, c) and 20 U/ml (d, e, f) of enzyme after 1, 2 and 3 day of degradation, magnification 3000x, scale 20 µm

Before degradation all of the fibres had a smooth surface. During the degradation process the surface of PLCL\_th\_1 fibres became coarser and projections were formed as a result of surface degradation. Subsequently, disintegration of the fibres took place. This morphological change explains why mass loss was faster than the decrease of the molar mass.

In Figure 20 on images c) and f) are seen fibres with high diameter which are not caused by a degradation process but it is cellulose fibres from filter paper. The degradation products were not possible to remove for their small quantity and sticking between fibres.

### 5.2.3 Degradation Study with 5 U/ml of Proteinase K

On the basis of the three days test with proteinase K enzyme, 5 U/ml of enzyme was the concentration selected for the following test. The experimental conditions were

the same as for the tests with 10 U/ml and 20 U/ml. Two samples of each material were prepared for each day and two negative control samples where the buffer (without enzyme addition) was changed every 24 hours. As in the previous experiments, mass loss, molar mass and surface morphology change were determined.

## Mass Loss

The mass loss profiles for the copolymers with application 5 U/ml of enzyme proteinase K is shown in Figure 21. Values for each day were averaged and plotted.

In this experiment, the copolymers did not demonstrate much difference in their mass loss profiles when compared with each other. A more significant change occurred after two days when the rate of mass loss of PLCL<sub>1</sub> began to significantly reduce, whilst for copolymer PLCL<sub>th\_1</sub> this effect occurred the next day. After four days, both copolymers had lost more than 90% of their initial weight.

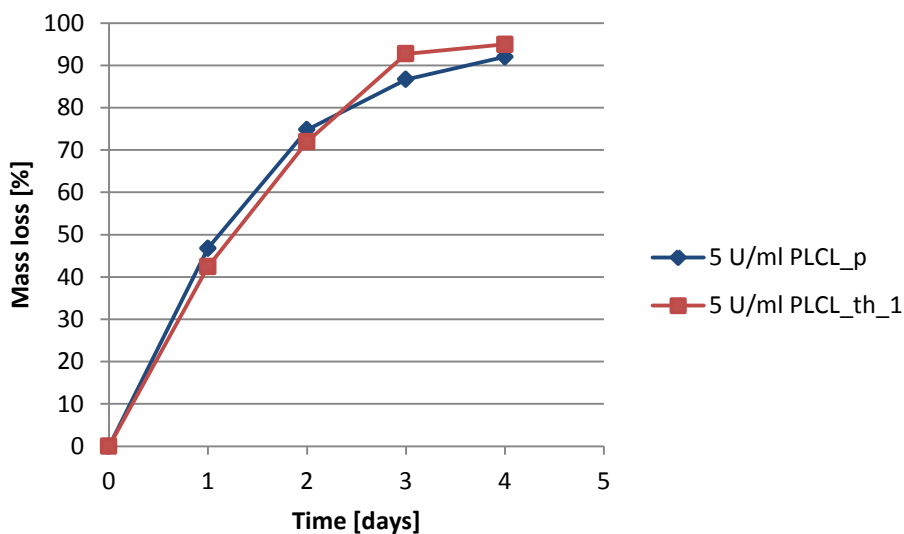


**Figure 21** Mass loss of PLCL with 5 U/ml of enzyme

## Molar Mass Change

The data for each day and the negative control sample are given in Table 9 changes in the molar mass of PLCL<sub>p</sub> and PLCL<sub>th\_1</sub> with 5 U/ml of enzyme are shown in Figure 22.

**Table 8** Molar mass loss with 5 U/ml of enzyme

Time [days]	PLCL_p		PLCL_th_1	
	M <sub>n</sub> [g/mol]	PDI [-]	M <sub>n</sub> [g/mol]	PDI [-]
0 day	73,600	1.81	35,100	1.70
1 day	50,000	2.42	26,500	1.93
2 day	20,800	5.21	23,000	1.98
3 day	7,200	1.80	3,000	1.42
4 day	6,300	1.985	-	-
Negative control sample	55,302	2.05	27,000	1.56

Progression of molar mass loss was different in the two materials. PLCL\_th\_1 had a lower rate of molar loss than PLCL\_p but this difference was no longer apparent by day three, when the materials had both lost 90 % of their initial molar mass. For small mass of PLCL\_th\_1 it was not possible to measure the number average molar mass after 4 days of the assay. Data for PLCL\_p after four days was obtained by dissolving the two samples to achieve the desired mass of 4 mg/ml for GPC analysis. This technique was not possible to use for PLCL\_th\_1 because the filter paper absorbed the majority of the remaining material.

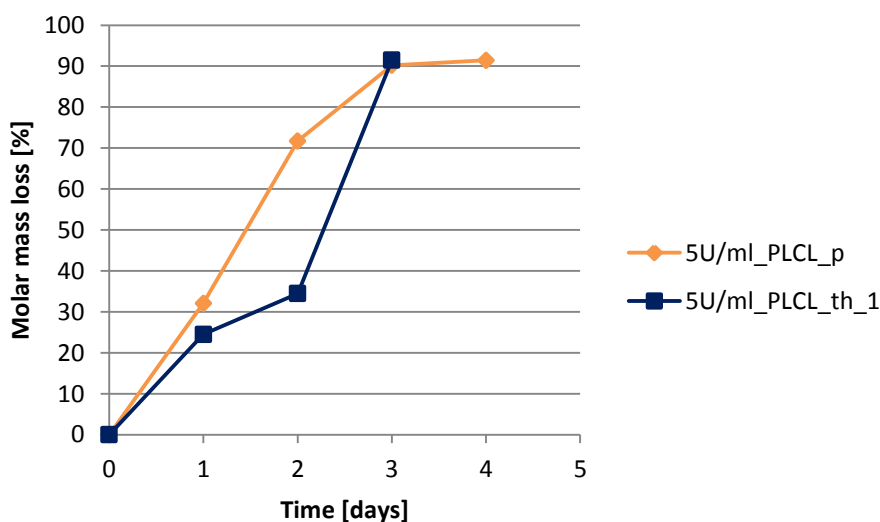


**Figure 22** Molar mass loss with 5 U/ml of enzyme

## Surface Morphology Change during Degradation

SEM provides a convenient method to follow the changes of surface morphology during degradation. The surface of PLCL\_p and PLCL\_th\_1 fibre layers are shown in Figure 23 and 24.

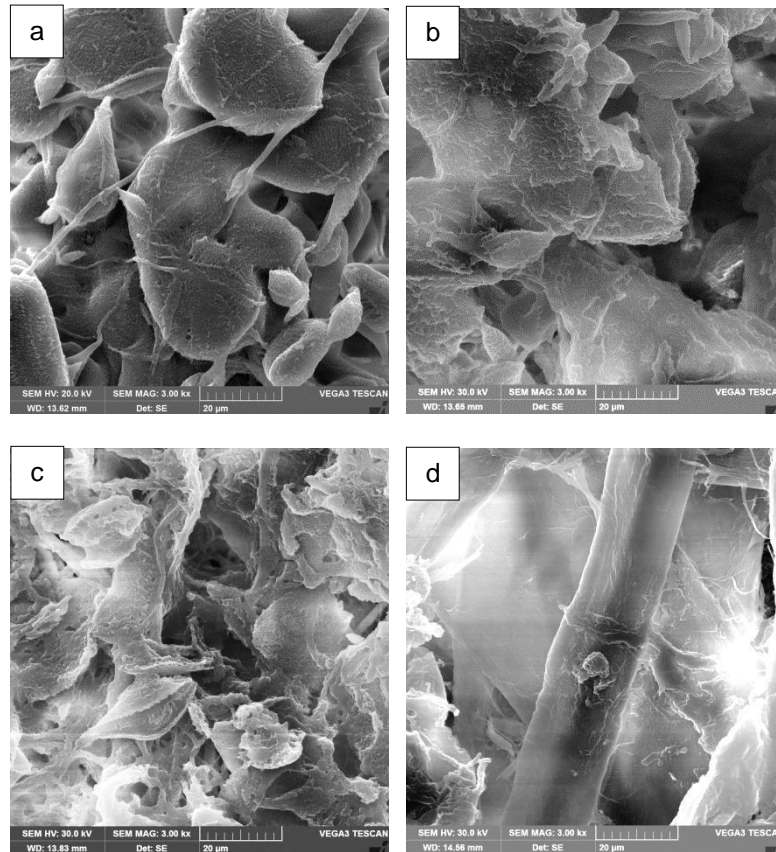


**Figure 23** SEM images of PLCL\_p with 5 U/ml of enzyme after 1 day (a), 2 day (b), 3 day (c) and 4 day (d), magnification 3000x, scale 20 µm

Figure 23 shows changes created after 4 days of treating the individual fabric layers with 5 U/ml of proteinase K. It can be seen that the surface change in the case of PLCL\_p are greatest while in PLCL\_th\_1 (Figure 24) are smaller as well as in experiment with 10 and 20 U/ml of enzyme.



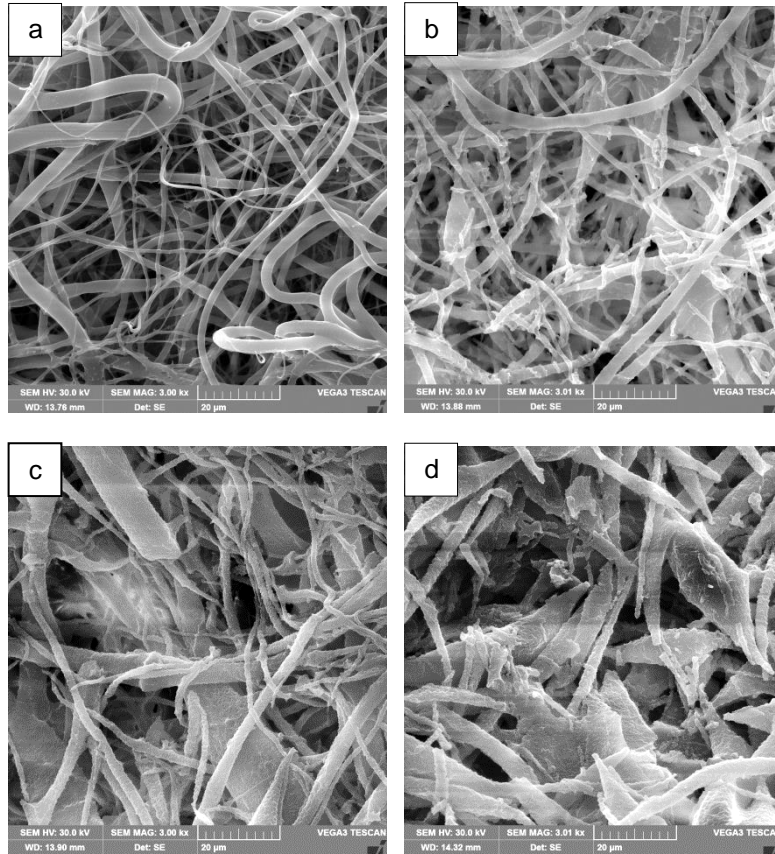


**Figure 24** SEM images of PLCL\_th\_1 with 5 U/ml of enzyme after 1 day (a), 2 day (b), 3 day (c) and 4 day (e), magnification 3000x, scale 20 μm

## Discussion

Biodegradable materials comprise a highly promising group of materials with a certain future in regenerative medicine. Polyesters have found their use in areas such as sewing threads, scaffolds and medical devices including catheters and stents. Their homopolymers have some disadvantages and therefore they are copolymerized and blended. By their copolymerization the mechanical properties, degradation rate and drug-reals properties can be controlled. Copolymer consists of flexible lactone units and rigid lactide units; thereby they are elastic and biodegradable materials suitable for scaffolds for tissue engineering. Kim and colleagues (2012) reported copolymer PLCL as a suitable material for vascular graft and cartilage. Their scaffolds were fabricated by a particulate leaching/extrusion method and by gel-spinning molding technique.

But the elastomeric properties have undue influence on electrospinning. Copolymers with the ratio 50 % of lactone become highly elastomeric and it is difficult to spin them. Kwon and colleagues (2005) deal with this issue in their study that focuses on the mechanical attributes of PLCL copolymers with various ratios.

Many authors stated that the leading indicator for the degradation rate is the length of the polymer chain, thus the molar mass. Others argue that in the case of the copolymer the main indicators are the mutual interactions linkages and randomness of distribution of the monomer in the copolymer (Liu, et al., 2009; (Lyu & Untereker, 2009). The length of the monomers in the chain is related to the crystallinity. Longer monomers increase the strength of the bonds and limit their movement; thereby they are increasing the crystallinity of the polymer. Copolymer with a higher molar mass and more random arrangement had faster degradation rate than the second copolymer. PLCL<sub>p</sub> degraded quicker and after 24 hours has lost its fibrous character. But this may be caused by the fibre diameter, which was lower than in case of PLCL<sub>th\_1</sub>. In further studies, it would be appropriate to compare the degradation rate of the film with fibres or fibres with the same diameters.

## Conclusion

The aim of thesis was the optimization of fibres production by electrospinning. Several copolymers from different suppliers were used. Materials differed in ratios of lactide and lactone monomers, molar mass distributions and alternation of monomers in the chain. These differences were confirmed by gel permeation chromatography and by nuclear magnetic resonance.

Several PLCL copolymers have failed to be optimized to fibres. Only foils and fused meshes originated instead. The degradation experiments were carried out only on two fibrous layers. These were copolymers with the similar ratio of lactide and lactone, but with random and blocky alternation of monomers and different molar mass.

The degradation experiments showed mass and molar mass losses. Clear evidence was shown in the SEM images of the morphological changes. Rate of mass loss did not match with the speed of change in molar mass, which is a consequence of the fibrous layer surfaces. Before the start of the degradation experiment, fibres had a smooth surface, but during the degradation began to coarsen and disintegrate. Mass loss is associated with macroscopic changes, while the change in molar mass is on a molecular level.

Enzymatic degradation is primarily a surface process and consequently it cannot be assumed that a reduction of molar mass occurred within the fibres. The variations experienced in the research for this thesis could have caused a buffer exchange when the sample part was removed with the buffer. Therefore, I propose to work on further experiments with heavier samples and instead of storing material in a direct contact with the media to use "extraction thimble." Thanks to the extraction thimble the material can be stored and access the buffer media at the same time. Another proposal is to reduce the amount of enzyme to be used in order to better estimate the trend changes. Also only pure buffer can be used, because even a negative control sample showed changes in molar mass loss after a week of experiment.

## Reference

- Agarwal, S., Mast, C., Dehnicke, K. & al., e., 2002. Rare earth metal initiated ring-opening polymerization of lactones. *Macromolecular rapid communications*, Issue 21, pp. 195-212.
- Agilent Technologies, 2001. *Agilent Technologies*. [Online]  
Available at:  
<https://www.chem.agilent.com/Library/technicaloverviews/Public/59882265.pdf>  
[Accessed 2014, October 6].
- Albertsson, A. C., 2002. *Degradable Aliphatic Polyesters*. Germany: Springer.
- Albertsson, A. C. & Eklund, M., 1995. Influence of Molecular Structure on the Degradation Mechanism of Degradable Polymers: In Vitro Degradation of Poly(trimethylene carbonate), Poly(trimethylene carbonate-co-caprolactone), and Poly(adipic anhydride). *Journal of Applied Polymer Science*, Issue 57, p. 87–103.
- Azom, 2011. *NMR Spectroscopy Analyzers: Azom*. [Online]  
Available at: <http://www.azom.com/materials-equipment.aspx?cat=115>  
[Accessed 2015, February 15].
- Bhat, S. V., 2005. *Biomaterials*. Harrow, UK: Alpha Science International Ltd..
- Brown, A. R., 2013. *Extreme Tissue Engineering : Concepts and Strategies for Tissue Fabrication*. Somerset, NJ, USA: John Wiley & Sons.
- Bruker, 2014. *Bruker: Products*. [Online]  
Available at: <http://www.bruker.com/products/mr/nmr.html>  
[Accessed 2014, November 11].
- Cohn, D. & Salomon, H., 2005. Designing biodegradable multiblock PCL/PLA thermoplastic elastomers. *Biomaterials*, Issue 26, pp. 2297-2305.
- Darensbourg, D., 2010. Ring-Opening Polymerization of l-Lactide and  $\epsilon$ -Caprolactone Utilizing Biocompatible Zinc Catalysts. Random Copolymerization of l-Lactide and  $\epsilon$ -Caprolactone. *Macromolecules*, Issue 43, pp. 8880-8886.
- Dimitrios, N. B., 2013. Nanocomposites of aliphatic polyesters: An overview of the effect of different nanofillers on enzymatic hydrolysis and biodegradation of polyesters. *Polymer Degradation and Stability*, Issue 98, pp. 1908-1928.
- Donglu, S., 2006. *Introduction to Biomaterials*. Beijing, China: Tsinghua University Press.
- Duda, A. & Penczek, S., 2002. Mechanisms of Aliphatic Polyester Formation. *Biopolymers: Polyesters II - Properties and Chemical Synthesis*, Issue 3b, pp. 371-430.

- Ducháček, V., 2006. *Polymery - výroba, vlastnosti, zpracování, použití*. Praha: VŠCHT Praha.
- Ebnesajjad, S., 2013. *Handbook of Biopolymers and Biodegradable Plastics: Properties, Processing, and Applications*. United States: Elsevier.
- Elias, H. G., 2005. *Macromolecules - Volume 1: Chemical Structures and Syntheses*. Weinham: Wiley-VCH.
- Fernández, J., Etxeberria, A. & Sarasua, J., 2012a. Synthesis, structure and properties of poly(L-lactide-co-ε-caprolactone) statistical copolymers. *Journal of the Mechanical Behavior of Biomedical Materials*, September, pp. 100-112.
- Fernández, J., Etxeberria, A., Ugartemendia, J. & al., e., 2012b. Effects of chain microstructures on mechanical behavior and aging of a poly(L-lactide-co-ε-caprolactone) biomedical thermoplastic-elastomer. *Journal of the Mechanical behavior of Biomedical Materials*, Issue 12, pp. 29-38.
- Garkhal, K., Verma, S. & Kumar, N., 2007. Fast Degradable Poly(L-lactide-co-ε-caprolactone) Microspheres for Tissue Engineering: Synthesis, Characterization, and Degradation Behavior. *Journal of Polymer Science: Part A Polymer Chemistry*, Issue 45, pp. 2755-2764.
- Grakhal, K., Verma, S., Honnalagadda, S. & Kumar, N., 2007. Fast Degradable Poly(L-lactide-co-ε-caprolactone) Microspheres for Tissue Engineering: Synthesis, Characterization, and Degradation Behaviour. *Journal of Polymer Science: Part A: Polymer Chemistry*, pp. 2755-2764.
- He, W., Feng, Y., Zuwei, M. & Ramakrishna, S., 2008. Polymers for Tissue Engineering. *Polymers for Biomedical Applications*, pp. 310-335.
- Chen, Q., Lianga, S. & Thouas, G. A., 2013. Elastomeric biomaterials for tissue engineering. *Progress in Polymer Science*, Issue 38, pp. 584-656.
- Jiao, M., Yang, K., Cao, J. & al., e., 2014. Designing and Charakterization of Poly(L-Lactide)/Poly(ε-Caprolactone) Multiblock Copolymers. *Journal of Macromolecular Science, Part B: Physics*, Issue 53, pp. 191-204.
- Jirsák, O. & Kalinová, K., 2003. *Netkané textilie*. Liberec: Technická univerzita v Liberci.
- Kim, S. H., Jung, Y., Kim, Y. H. & Kim, S. H., 2012. Mechano-active scaffolds. V: G. Khang, editor *Handbook of Intelligent Scaffolds for Tissue Engineering and Regenerative Medicine*. Florida: Pan Stanford Publishing, pp. 568-590.
- Kwon, K., Kidoaki, S. & Matsuda, T., 2005. Electrospun nano- to microfiber fabrics made of biodegradable copolyesters: structural characteristics, mechanical properties and cell adhesion potential. *Biomaterials*, Issue 26, p. 3929–3939.

- Labet, M. & Thielemans, W., 2009. Synthesis of polycaprolactone: a review. *Chemical Society Reviews*, Svazek 38, pp. 3484-3504.
- Lanza, R., Langer, R. & Vacanti, J., 2014. *Principles of Tissue Engineering*. London: Elsevier.
- Larrañaga, A., Diamanti, E., Rubio, E. & al., e., 2014a. A study mechanical properties and cytocompatibility of lactide and caprolactone based scaffolds with inorganic bioactive particles. *Material Science and Engineering C*, Issue 42, pp. 451-460.
- Larrañaga, A., Aldazabal, P., Martin, F. & al., e., 2014b. Hydrolytic degradation and bioactivity of lactide and caprolactone based sponge-like scaffolds loaded with bioactive glass particles. *Polymer Degradation and Stability*, Issue 110, pp. 120-128.
- Liu, F., Zhao, Z., Yang, J. & et al., 2009. Enzyme-catalyzed degradation of poly(l-lactide)/poly(caprolactone) diblock, triblock and four-armed copolymers. *Polymer Degradation and Stability*, Issue 94, p. 227-233.
- Lopes, M. S., Jardini, A. L. & Filho, R. M., 2012. Poly (lactic acid) production for tissue engineering. *Procedia Engineering*, Issue 42, pp. 1402-1413.
- Lukáš, D., Martinová, L., Amler, E. & et al., 2008. *Lékařské textilie*. Prague, Czech Republic: Asociace inovačního podnikání ČR.
- Lyu, S. & Untereker, D., 2009. Degradability of Polymers for Implantable Biomedical Devices. *International Journal of Molecular Sciences*, Issue 10, pp. 4033-4065.
- Macomber, R. S., 1998. *A Complete Introduction to Modern NMR Spectroscopy*. New Jersey: John Wiley & Sons.
- Miller, M. J., 2005. *Chromatography: Concepts and Contrasts*. New Jersey: John Wiley and Sons.
- Mitpuppatham, C., Nithitanaku, M. & Supaphol, P., 2004. Ultrafine electrospun polyamide-6 fibers, effect of solution conditions on morphology and average fiber diameter. *Macromolecular Chemistry and Physics*, November, pp. 2327-2338.
- Nair, L. S. & Laurencin, C. T., 2007. Biodegradable polymers as biomaterials. *Progress in Polymer Science*, Issue 32, pp. 762-798.
- Nampoothiri, K. M., Nair, N. R. & John, R. P., 2010. An overview of the recent developments in polylactide (PLA) research. *Bioresource Technology*, Issue 101, pp. 8493-8501.
- NMR laboratoř PŘF MU, 2014. *NMR laboratoř*. [Online] Available at: <http://nmrlab.chemi.muni.cz/img/NMR.pdf> [Accessed 2014, December 11].

- Peponi, L., Fernández, A. M. & Kenny, J. M., 2012. Nanostructured morphology of a random P(DLLA-co-CL) copolymer. *Nanoscale Research Letters*, Issue 7, pp. 1-7.
- Petruš, J., 2011. *ChemPoint*. [Online]  
Available at: <http://www.chempoint.cz/kyselina-polymlečna-nején-jako-biodegradabilní-polymer>. [Accessed 2015, April 10].
- Ramakrishna, S., Fujihara, K., Teo, W. E. & et al., 2005. *An Introduction to Electrospinning and Nanofibers*. Singapore: World Scientific Publishing Co. Pte. Ltd.
- Rui, L. R. & Román, J., 2005. *Biodegradable Systems in Tissue Engineering and Regenerative Medicine*. CRC Press.
- Sigma-Aldrich, 2014. *Sigma-Aldrich: Data Sheet*. [Online]  
Available at: <http://www.sigmaaldrich.com/content/dam/sigma-aldrich/docs/Sigma-Aldrich/Datasheet/p2308dat.pdf>  
[Accessed 2015 April 9].
- Stanger, J., Tucker, N. & Staiger, M., 2005. *Electrospinning*. Shawbury, UK: Smithers Rapra Technology.
- Tiwari, A. & Srivastava, R. B., 2012. *Biotechnology in Biopolymers: Developments - Applications and Challenging Areas*. Shawbury: Smithers Rapra Technology.
- University of Cambridge, 2011. *Copolymers: University of Cambridge*. [Online]  
Available at: [http://www.doitpoms.ac.uk/tlplib/polymerbasics/co\\_polymers.php](http://www.doitpoms.ac.uk/tlplib/polymerbasics/co_polymers.php)  
[Accessed 2015, April 25].
- Vieira, A. C., Vieira, J. C., Ferra, J. M. & et al., 2011. Mechanical study of PLA-PCL fibers during in vitro degradation. *Journal of the Mechanical Behaviour of Biomedical Materials*, pp. 451-460.
- Warwick Scientific Services, 2012. *GPC: Warwick Scientific Services*. [Online]  
Available at: <http://www2.warwick.ac.uk/services/ris/business/analyticalguide/gpc/>  
[Accessed 2014, December 15].
- Waters, 2012. *Waters, the science what's possible - GPC, Gel permeation chromatography*. [Online]  
Available at: [http://www.waters.com/waters/en\\_CZ/GPC---Gel-Permeation-Chromatography/nav.htm?cid=10167568&locale=en\\_CZ](http://www.waters.com/waters/en_CZ/GPC---Gel-Permeation-Chromatography/nav.htm?cid=10167568&locale=en_CZ)  
[Accessed 2014, September 10].
- Wendorff, J. H., Agarwal, S. & Greiner, A., 2012. *Electrospinning - Materials, Processing, Applications*. Singapore: Wiley-VCH Verlag & Co. KGaA.
- Yu, T., Ren, J., Gu, S. & et al., 2010. Preparation and characterization of biodegradable poly(lactic acid)-block-poly( $\epsilon$ -caprolactone) multiblock copolymer. *Polymers Advanced Technologies*, pp. 183-188.

Zenkiewicz, M., Richert, A., Malinowski, R. & et al., 2013. A comparative analysis of mass losses of some aliphatic polyesters upon enzymatic degradation. *Polymer Testing*, Issue 32, pp. 209-214.



## List of Appendix

**Appendix 1** *Molar masses of copolymer granules*

**Appendix 2** *Data sheets of commercial products*

**Appendix 3** *<sup>1</sup>H NMR spectrum of PLCL copolymers*

**Appendix 4** *Fibre diameters and histograms*

**Appendix 5** *Measurement of fibre diameters*

**Appendix 6** *Table of sample weights specified for degradation experiment*

**Appendix 5** *0.1 M Tris buffer composition*

## Appendix 1 Molar masses of copolymer granules

Sample name	Refractive index detector			Ultraviolet detector		
	M <sub>w</sub> [g/mol]	M <sub>n</sub> [g/mol]	PDI [-]	M <sub>w</sub> [g/mol]	M <sub>n</sub> [g/mol]	PDI [-]
PLCL_p	193,000	94,900	2.03	1,027,000	118,500	8.67
PLCL_th_1	93,500	48,900	1.91	45,200	3,400	1.35
PLCL_th_2	122,900	69,800	1.76	48,600	15,900	3.05
PLCL_th_3	54,000	30,000	1.78	114,400	13,400	8.54
PLCL_pls	90,800	47,900	1.90	-	-	-
P(L)CL_pls	77,000	47,400	1.62	-	-	-

## Appendix 2 Data sheets of commercial products

### PLCL\_p



Product data sheet

Rev. No. 5 / October 2012

## PURASORB<sup>®</sup> PLC 7015

**Description** PURASORB PLC 7015 is a GMP grade copolymer of L-lactide and  $\epsilon$ -caprolactone in a 70/30 molar ratio and with an inherent viscosity midpoint of 1.5 dl/g. It is supplied in the form of white to light tan granules. PURASORB PLC 7015 is primarily used for medical device applications and is suitable for all commonly used polymer processing techniques.

Specification	Test	Method	Specification
Appearance	Appearance	visual	white to light tan granules
Identification	Identification	FTIR	conforms to reference
L-lactide content	L-lactide content	HNMR	67 - 73 mol%
Caprolactone content	Caprolactone content	HNMR	33 - 27 mol%
Inherent viscosity	Inherent viscosity	CHCl <sub>3</sub> , 25°C, 0.1 g/dl	1.2 - 1.8 dl/g
Residual monomer	Residual monomer	GC	max. 0.5 wt. %

For each batch a certificate of analysis is provided, showing the analytical data determined in our quality control laboratory. Additional analytical data can be made available upon request.

Physical-chemical properties	Molecular formula	(C <sub>6</sub> H <sub>8</sub> O <sub>4</sub> *C <sub>6</sub> H <sub>10</sub> O <sub>2</sub> ) <sub>n</sub>
Chemical name	Chemical name	(3S-cis)-3,6-dimethyl-1,4-dioxane-2,5-dione, polymer with 2-oxepanone
CAS Registry number	CAS Registry number	65408-67-5

**Packaging** PURASORB PLC 7015 can be supplied in 1 or 5 kg packages. Normal packaging consists of an inner bag of clean room grade PE and an outer bag of aluminum coated polyester-PE laminate. The packed product is shipped in an additional bag of PE and in PE containers for added protection.

**Storage & Handling** When stored in the original packaging at low temperatures (-15°C), PURASORB PLC 7015 keeps its initial properties for five years.

Allow the material to reach room temperature before opening the packaging. After opening the original packaging PURASORB PLC 7015 is best stored in an inert atmosphere and at low temperatures (-15°C).

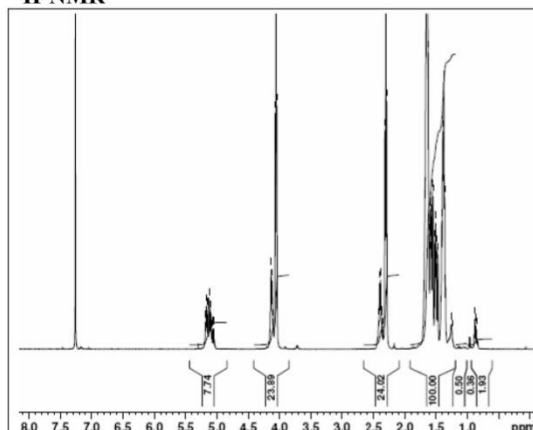
## PLCL\_pls

**No. AP74**

## Certificate of Analysis

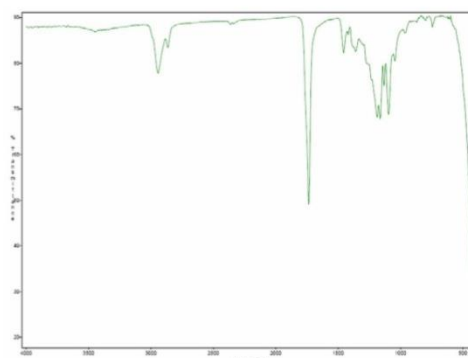
Product Name: Poly(L-Lactic-co-caprolactone) copolymer ester endcap (30:70 LA:CL, Mn: 45,000-55,000 Da) (Lot#: 30315JSG)

### H-NMR



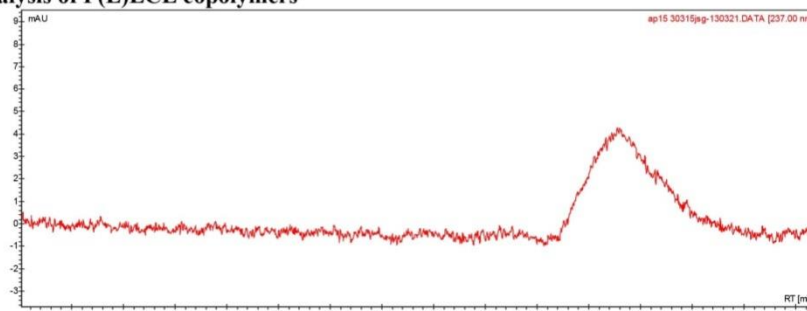
H-NMR Spectrum of P(L)LCL copolymers in CDCl<sub>3</sub> (Varian Inova 500 MHz instrument), NMR of P(L)LCL copolymers: LA/CL = 29%/71%

### FTIR



Analysis Method: Collected from cast-film on KBR salt-plate placed in Satellite FTIR (Thermo-Mattson) and analyzed in transmission mode.

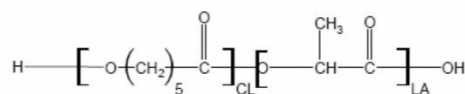
- GPC analysis of P(L)LCL copolymers**



Analysis Method: Varian Prostar system with 1 ml/min DCM flow across two Phenogel 5u columns and one PLGel Resipore column (Agilent). Detection via UV/Vis, calibrated against polystyrene standards

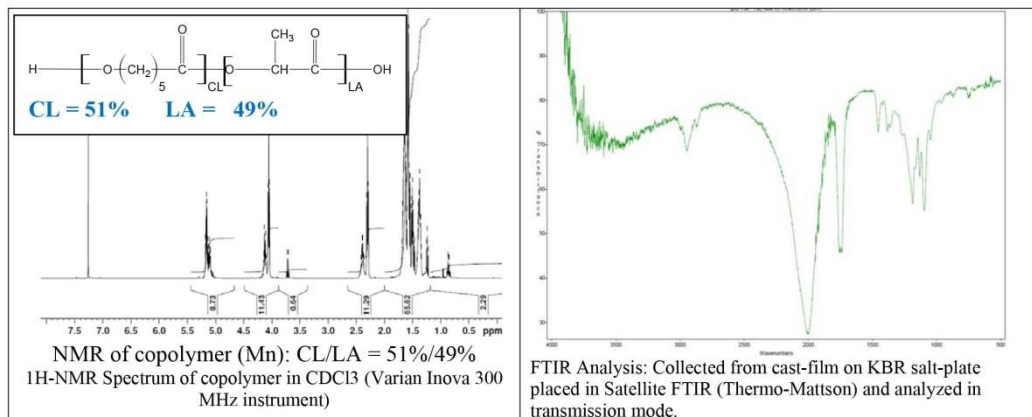
Polymer	Mn (from GPC)	Mw (from GPC)	PDI
P(L)LCL	52955	77867	1.47

- Structure of P(L)LCL copolymers**

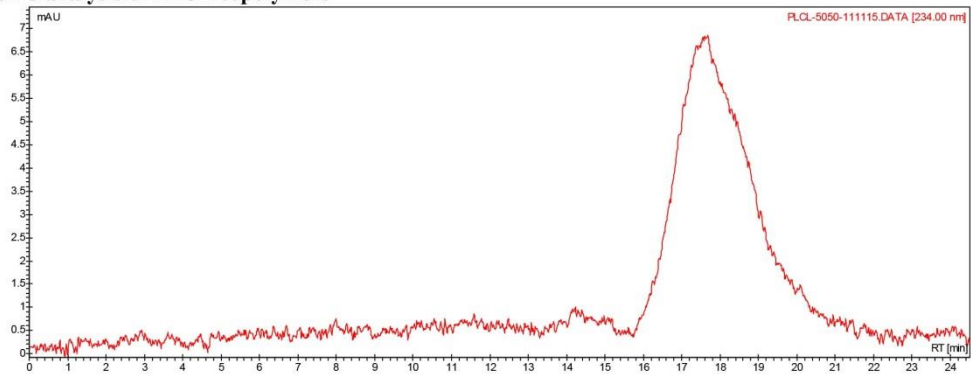


## No. AP67 Certificate of Analysis

Product Name: Poly(L-Lactic-co-caprolactone) Copolymer (50:50) (Mn 45k-65kDa)



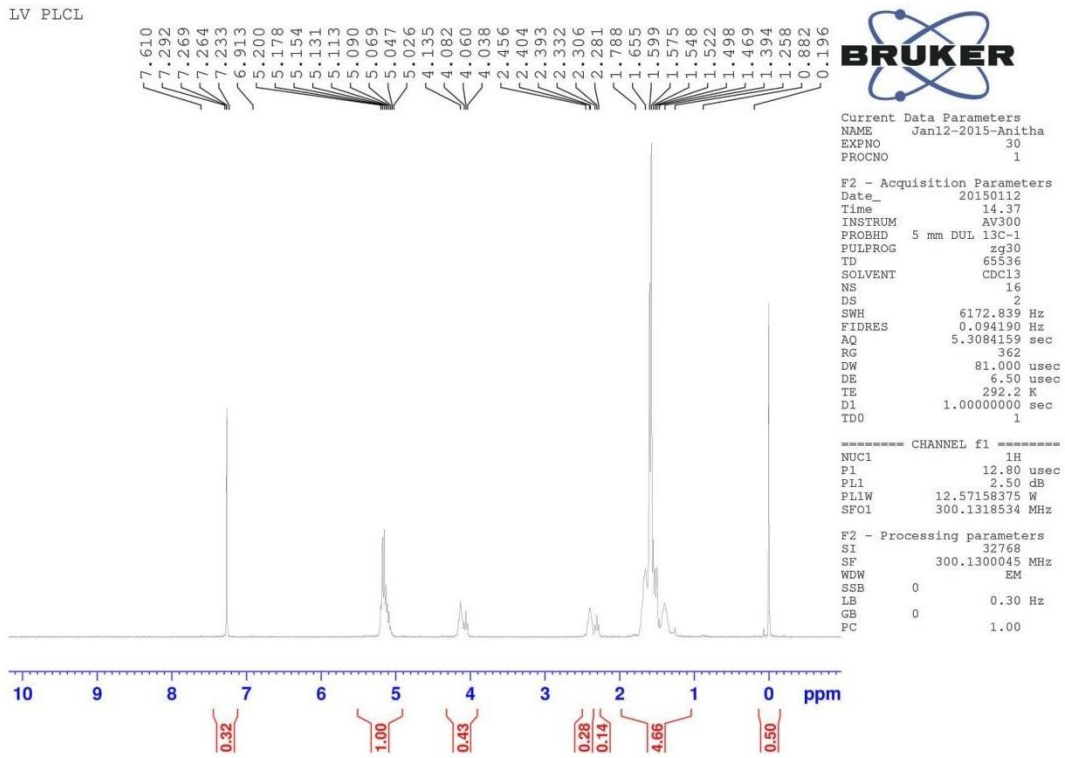
- GPC analysis of PLCL copolymers



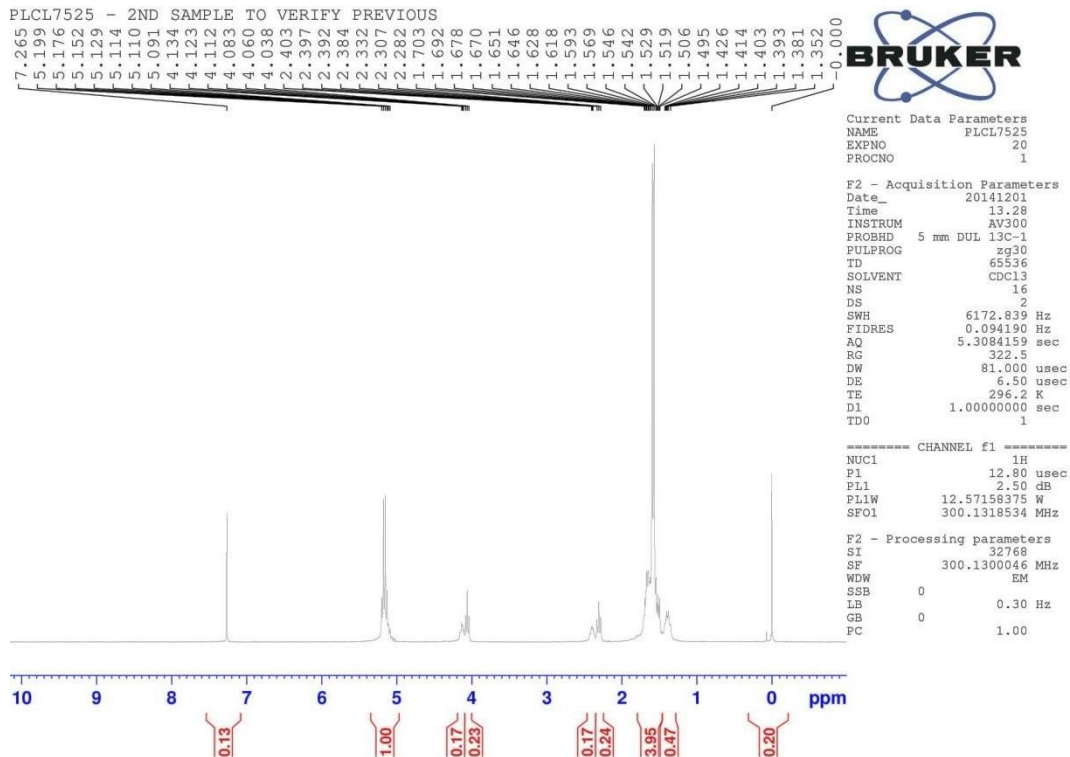
Analysis Method: Varian Prostar system with 1 ml/min DCM flow across two Resipore 3 um columns and one Mixed E column (Varian) and with UV-Vis (PDA) detection. Calibrated against polystyrene standards

Polymer	Mn (from GPC)	Mw (from GPC)	PDI
PLLCL	48639	79896	1.64

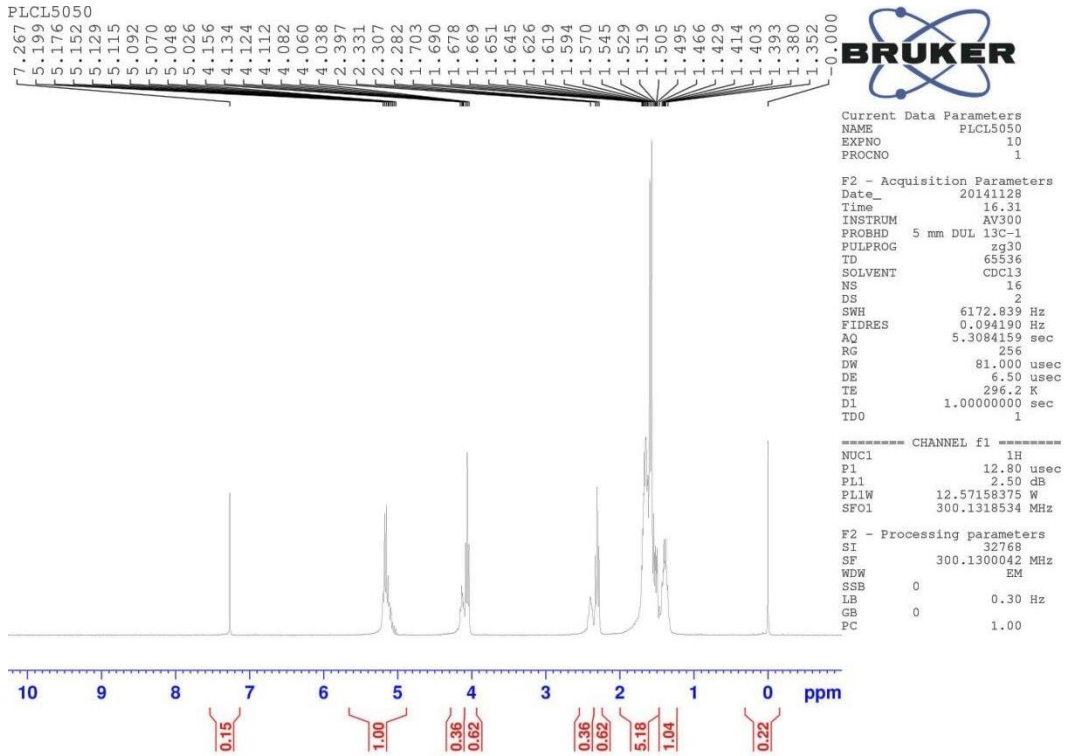
# Appendix 3 $^1\text{H}$ NMR spectrum of PLCL copolymers



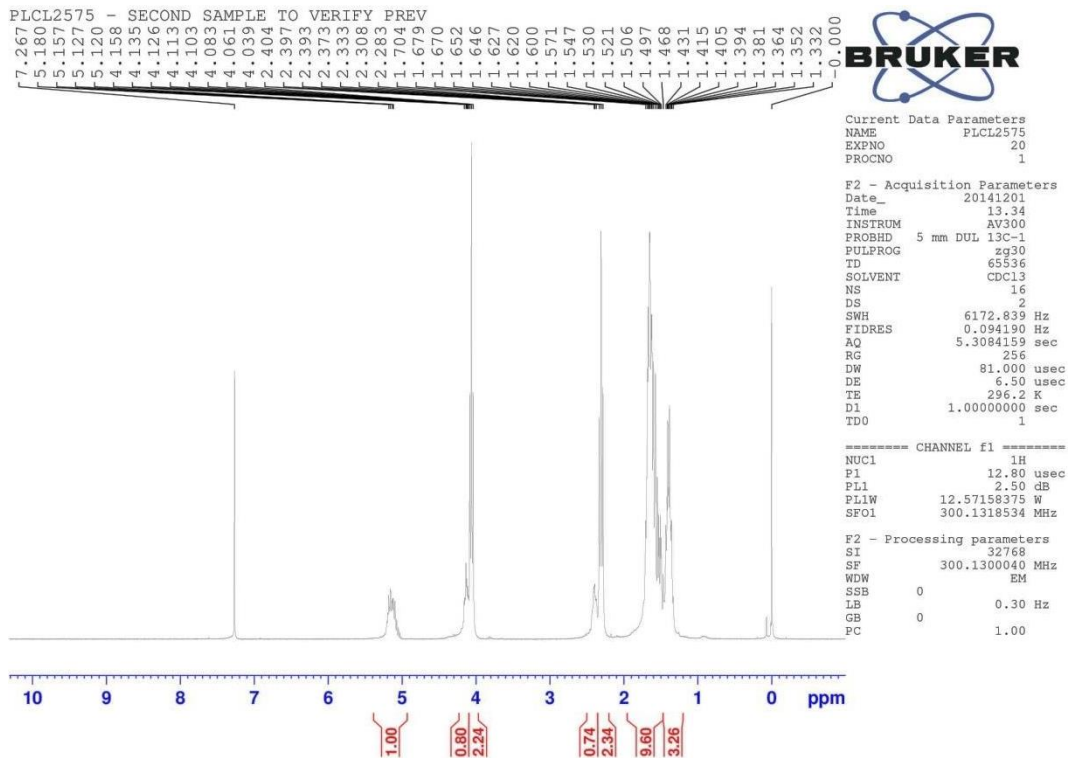
$^1\text{H}$  NMR spectrum of PLCL<sub>p</sub>



$^1\text{H}$  NMR spectrum of PLCL<sub>th\_1</sub>

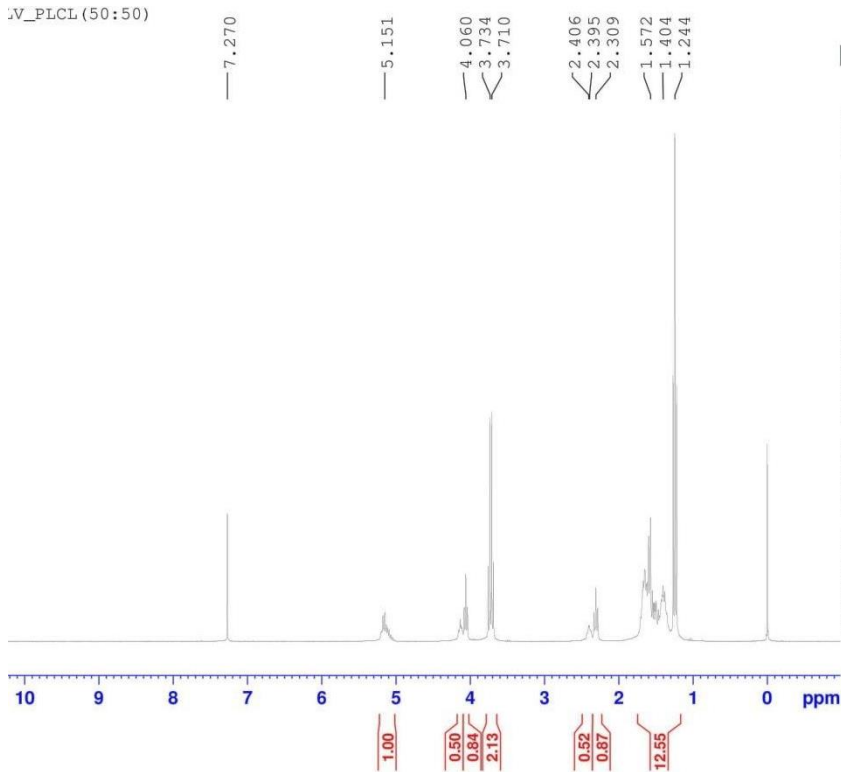


<sup>1</sup>H NMR spectrum of PLCL\_th\_2



<sup>1</sup>H NMR spectrum of PLCL\_th\_3

LV\_PLCL (50:50)



Current Data Parameters  
 NAME Apr13-2015-Pre  
 EXPNO 10  
 PROCNO 1

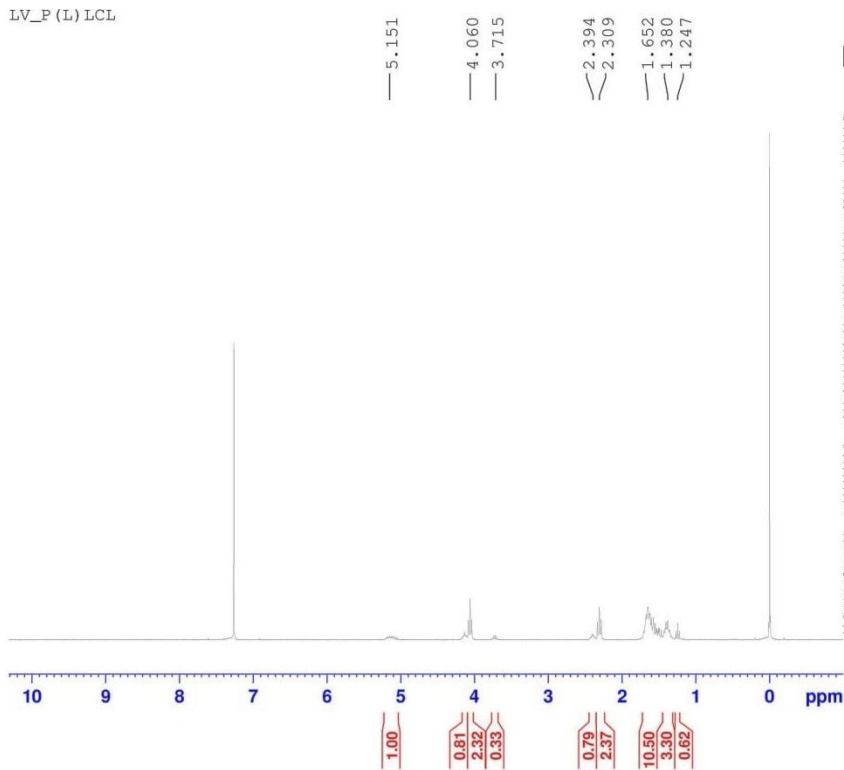
F2 - Acquisition Parameters  
 Date\_ 20150413  
 Time 15.43  
 INSTRUM AV300  
 PROBHD 5 mm DUL 13C-1  
 PULPROG zg30  
 TD 65536  
 SOLVENT CDCl3  
 NS 16  
 DS 2  
 SWH 6172.839 Hz  
 FIDRES 0.094190 Hz  
 AQ 5.3084159 sec  
 RG 256  
 DW 81.000 usec  
 DE 6.50 usec  
 TE 293.2 K  
 D1 1.00000000 sec  
 TDO 1

----- CHANNEL f1 -----  
 NUC1 1H  
 P1 10.81 usec  
 PL1 2.50 dB  
 PL1W 12.57158375 W  
 SF01 300.1318534 MHz

F2 - Processing parameters  
 SI 32768  
 SF 300.1300032 MHz  
 WDW EM  
 SSB 0  
 LB 0.30 Hz  
 GB 0  
 PC 1.00

<sup>1</sup>H NMR spectrum of PLCL\_pls

LV\_P (L) LCL



Current Data Parameters  
 NAME Apr13-2015-Pre  
 EXPNO 20  
 PROCNO 1

F2 - Acquisition Parameters  
 Date\_ 20150413  
 Time 15.50  
 INSTRUM AV300  
 PROBHD 5 mm DUL 13C-1  
 PULPROG zg30  
 TD 65536  
 SOLVENT CDCl3  
 NS 16  
 DS 2  
 SWH 6172.839 Hz  
 FIDRES 0.094190 Hz  
 AQ 5.3084159 sec  
 RG 645.1  
 DW 81.000 usec  
 DE 6.50 usec  
 TE 293.2 K  
 D1 1.00000000 sec  
 TDO 1

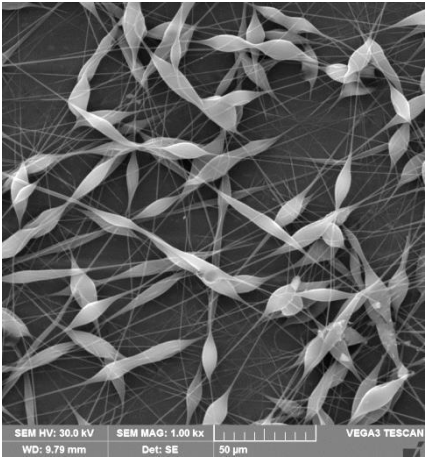
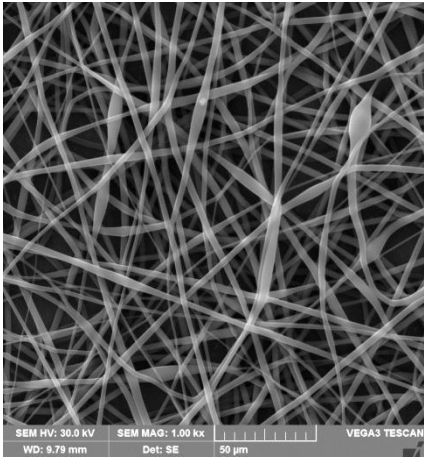
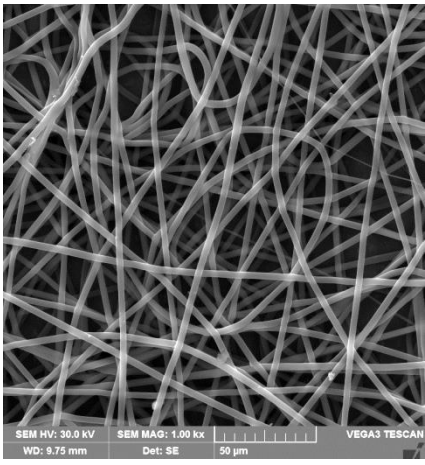
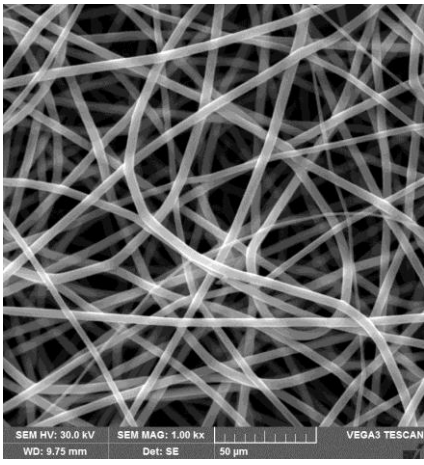
----- CHANNEL f1 -----  
 NUC1 1H  
 P1 10.81 usec  
 PL1 2.50 dB  
 PL1W 12.57158375 W  
 SF01 300.1318534 MHz

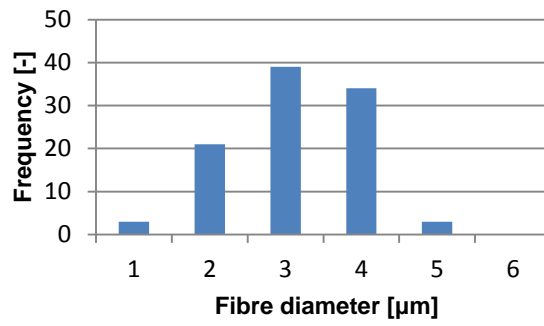
F2 - Processing parameters  
 SI 32768  
 SF 300.1300056 MHz  
 WDW EM  
 SSB 0  
 LB 0.30 Hz  
 GB 0  
 PC 1.00

<sup>1</sup>H NMR spectrum of P(L)CL\_pls

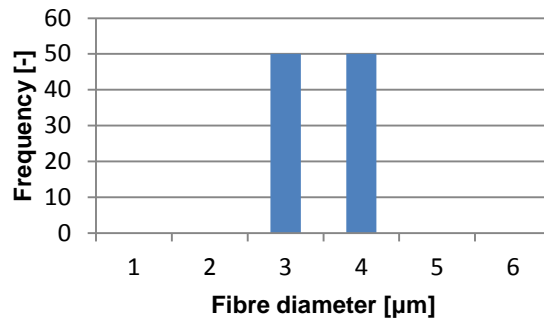


## Appendix 4 Fibre diameters and histograms

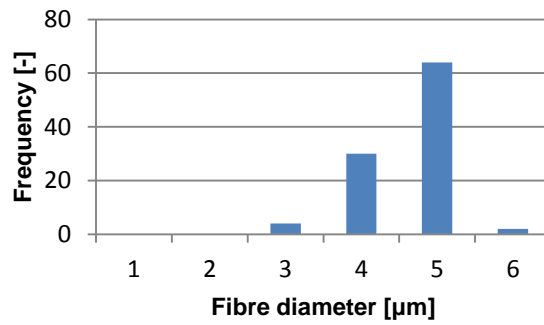
PLCL_th_1, magnification 1000x, scale 50 $\mu\text{m}$			
12 wt %		14 wt %	
			
Mean [ $\mu\text{m}$ ]	-	Mean [ $\mu\text{m}$ ]	2.64
SD [ $\mu\text{m}$ ]	-	SD [ $\mu\text{m}$ ]	0.83
Min [ $\mu\text{m}$ ]	-	Min [ $\mu\text{m}$ ]	0.62
Max [ $\mu\text{m}$ ]	-	Max [ $\mu\text{m}$ ]	4.56
16 wt %		20 wt %	
			
Mean [ $\mu\text{m}$ ]	3.01	Mean [ $\mu\text{m}$ ]	4.13
SD [ $\mu\text{m}$ ]	0.30	SD [ $\mu\text{m}$ ]	0.50
Min [ $\mu\text{m}$ ]	2.33	Min [ $\mu\text{m}$ ]	2.71
Max [ $\mu\text{m}$ ]	3.75	Max [ $\mu\text{m}$ ]	5.57



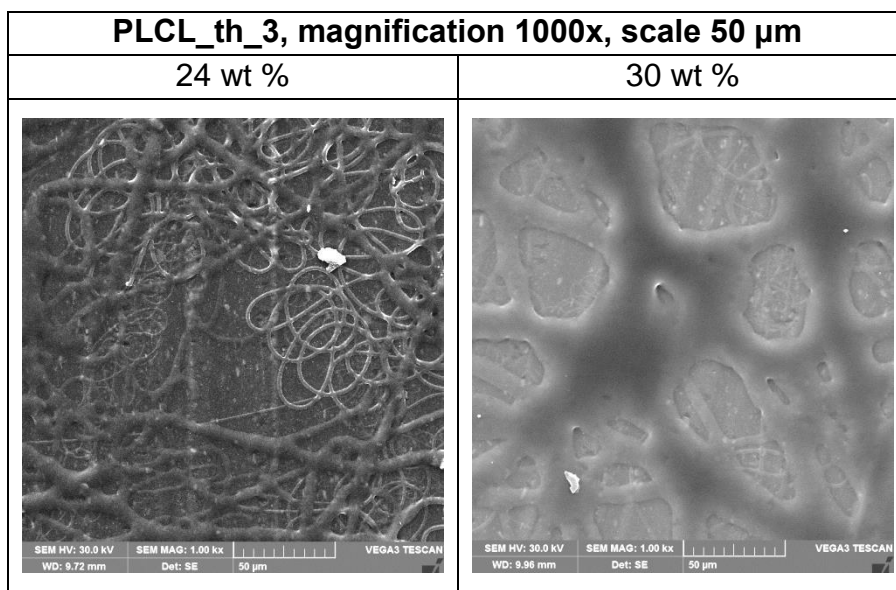
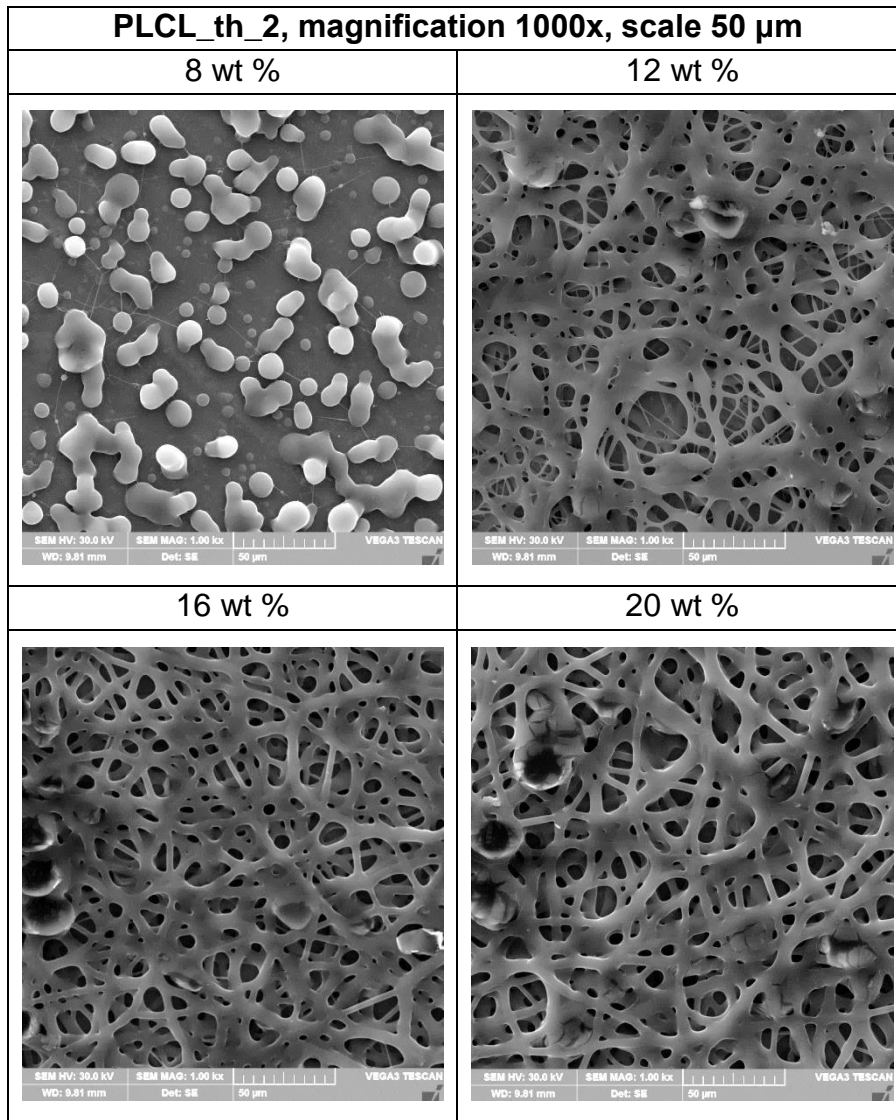
*Histogram of 14 wt % PLCL\_th\_1*



*Histogram of 16 wt % PLCL\_th\_1*



*Histogram of 20 wt % PLCL\_th\_1*



## Appendix 5 Measurement of fibre diameters

<b>PLCL_p</b>			
0.801	0.614	0.485	0.397
1.105	0.508	0.655	0.296
0.771	0.488	0.914	0.479
0.595	0.602	0.533	0.949
1.52	0.648	0.541	0.584
1.176	0.511	0.609	0.51
0.457	0.651	0.572	0.388
0.7	0.58	0.497	0.401
0.762	0.421	0.541	0.468
0.681	0.539	0.392	0.401
0.381	0.241	0.572	0.508
0.549	0.539	0.345	0.483
0.58	0.53	0.549	0.69
0.657	0.497	0.41	0.438
0.434	0.485	0.269	0.611
0.511	0.381	0.444	0.388
0.345	0.541	0.595	0.518
0.583	0.508	0.533	0.359
0.993	0.497	0.657	0.508
1.351	0.549	0.862	0.309
1.186	0.628	0.756	0.296
0.562	0.666	0.323	0.406
0.614	0.723	0.511	1.001
0.7	0.554	0.467	0.777
0.421	0.434	0.375	0.241
<b>Mean [µm]</b>	<b>0.576</b>		
<b>Standard deviation[µm]</b>	<b>0.223</b>		
<b>Min [µm]</b>	<b>0.241</b>		
<b>Max [µm]</b>	<b>1.52</b>		

<b>PLCL_th_1</b>			
2.415	1.777	2.57	2.988
2.961	1.795	2.093	2.734
2.494	2.57	1.848	2.699
4.615	1.703	1.908	2.334
2.415	2.154	1.804	2.191
0.767	2.717	2.22	3.052
0.828	1.402	1.544	1.534
0.483	0.483	2.334	1.544
0.628	0.324	1.908	1.544
1.85	0.458	1.933	1.655
1.874	1.077	2.031	1.149
1.755	0.523	1.795	1.606
1.505	1.081	1.942	1.655
0.404	0.852	2.341	1.694
0.404	0.37	4.991	1.257
3.577	0.628	1.241	0.898
1.241	0.701	0.571	0.324
0.819	4.309	1.346	0.449
1.831	4.253	0.602	0.508
1.914	1.733	0.539	0.381
0.539	1.724	0.862	0.701
1.077	1.051	1.353	0.458
2.895	0.523	1.333	0.635
1.795	1.768	1.643	1.247
1.447	1.942	2.838	1.11
<b>Mean [μm]</b>	<b>1.624</b>		
<b>Standard deviation[μm]</b>	<b>0.972</b>		
<b>Min [μm]</b>	<b>0.324</b>		
<b>Max [μm]</b>	<b>4.991</b>		

**Appendix 6** Table of samples weights specified for degradation experiment

<b>PLCL_p</b>					<b>PLCL_th_1</b>			
<b>10 U/ml</b>					<b>10 U/ml</b>			
<b>Degrad. day</b>	<b>Sample name</b>	<b>Sample weight [mg]</b>	<b>Sample weight after degradation [mg]</b>	<b>Mass loss [%]</b>	<b>Sample name</b>	<b>Sample weight [mg]</b>	<b>Sample weight after degradation [mg]</b>	<b>Mass loss [%]</b>
1 day	<b>1p</b>	48.83	29.27	40.7	<b>1th</b>	49.57	32.37	34.70
2 day	<b>2p</b>	50.20	12.87	76.86	<b>2th</b>	50.73	16.47	67.54
	<b>3p</b>	47.77	9.87		-	-	-	-
3 day	-	-	-	-	<b>3th</b>	48.77	1.33	97.27
<b>20 U/ml</b>					<b>20 U/ml</b>			
1 day	<b>4p</b>	48.93	30.50	37.67	<b>4th</b>	49.60	32.27	34.95
2 day	<b>5p</b>	50.00	13.67	80.48	<b>5th</b>	49.73	14.97	69.91
	<b>6p</b>	50.73	5.93	88.30	-	-	-	-
3 day	-	-	-	-	<b>6th</b>	49.07	0.53	98.91
<b>5 U/ml</b>					<b>5 U/ml</b>			
Negat. control sample	<b>K1_p</b>	51.13	51.50	-0.72	<b>K1_th</b>	50.17	49.37	1.59
	<b>K2_p</b>	50.17	53.03	-5.71	<b>K2_th</b>	49.73	50.57	-1.68
1 day	<b>7p</b>	50.97	25.80	49.38	<b>7th</b>	50.13	28.77	42.62
	<b>8p</b>	46.87	26.17	44.17	<b>8th</b>	48.60	28.10	42.18
2 day	<b>9p</b>	50.16	13.20	73.68	<b>9th</b>	50.43	12.73	74.75
	<b>10p</b>	49.07	11.83	75.88	<b>10th</b>	50.10	15.47	69.13
3 day	<b>11p</b>	50.03	9.27	81.48	<b>11th</b>	50.30	3.10	93.84
	<b>12p</b>	50.33	4.10	91.85	<b>12th</b>	50.33	4.23	91.59
4 day	<b>13p</b>	50.83	8.93	82.43	<b>13th</b>	50.87	2.10	95.87
	<b>14p</b>	48.27	4.67	90.33	<b>14th</b>	50.07	2.83	94.34
	<b>15p</b>	50.20	4.40	91.24	<b>15th</b>	49.87	2.60	94.79
	<b>16p</b>	51.11	2.83	94.46	<b>16th</b>	50.57	2.10	95.85
	<b>17p</b>	50.37	5.83	88.42	<b>17th</b>	49.93	2.53	94.93
	<b>18p</b>	49.03	0.80	98.37	<b>18th</b>	50.57	2.80	94.46
	<b>19p</b>	49.10	3.80	92.26	<b>19th</b>	50.87	2.30	95.48
<b>20p</b>	47.77	5.30	88.90	<b>20th</b>	49.27	2.93	94.05	

## **Appendix 7** *0.1 M Tris buffer composition*

Preparation of 1 litre of 0.1 M Tris buffer

- 800 ml distilled water (after mixing of all components add water to 1 litre)
- 12.14 g Tris
- hydrochloric acid (HCl) to adjust the pH = 8
- 0.2 g Sodium nitride ( $\text{Na}_3\text{N}$ )